Journal of Marine Systems
April 2022, Volume 228, Pages 103693 (17p.)
https://doi.org/10.1016/j.jmarsys.2021.103693
https://archimer.ifremer.fr/doc/00741/85281/

Origin and fate of long-chain polyunsaturated fatty acids in the Kerguelen Islands region (Southern Ocean) in late summer

Remize Marine [1, 2], Planchon Frederic [1, *], Loh Ai Ning [2], Grand Fabienne Le [1], Bideau Antoine [1], Puccinelli Eleonora [1], Volety Aswani, Soudant Philippe [1, *]

[1] Univ. Brest, CNRS, IRD, Ifremer, UMR 6539 LEMAR, F-29280 Plouzané, France
[2] University of North Carolina Wilmington, Department of Earth and Ocean Sciences, Center for Marine Science, 5600 Marvin K. Moss Ln, Wilmington, NC 28403, USA
[3] Elon University, 50 Campus Drive, Elon, NC 27244, USA

* Corresponding authors : Frédéric Planchon, email address : frederic.planchon@univ-brest.fr ; Philippe Soudant, email address : philippe.soudant@univ-brest.fr

Abstract :

Abstract Long-chain polyunsaturated fatty acids (LC-PUFA) are molecules produced at the basis of marine food webs and essential for ecosystem functioning. This study reports detailed fatty acid (FA) composition including the two LC-PUFA 20:5n-3 and 22:6n-3, in suspended organic matter (SPOM) from the upper 300 m collected in the Kerguelen Island region in the Southern Ocean during the post-bloom period (February–March 2018; project MOBYDICK). FA profiles were largely dominated by PUFA (53–69% of Total Fatty Acid, TFA) regardless of stations and among PUFA, proportions of LC-PUFA were especially high, making up 27–44% of TFA both in the ML and upper mesopelagic. 20:5n-3 and 22:6n-3 co-occurred in the ML as a result of the post-bloom phytoplankton community showing a mixed composition dominated by small size phytoplankton (prymnesiophytes and prasinophytes) supplying 22:6n-3, and with diatoms in lower proportions supplying 20:5n-3. Elevated levels of LC-PUFA were observed both inside the iron-fertilized area on the Kerguelen Plateau and downstream, and outside in High Nutrient Low Chlorophyll waters located upstream of the Plateau, and appeared unrelated to site. In the upper mesopelagic, both LC-PUFA were maintained at high relative proportions suggesting an efficient and possibly fast vertical transfer from the surface. Transfer with depth seems to proceed via distinct pathways according to LC-PUFA. 20:5n-3 may be exported along with diatoms, presumably in the form of large intact cells, aggregates as well as resting spores. For 22:6n-3, transfer may involve a channeling through the heterotrophic food web resulting in its association with fecal material at depth. Channeling of 22:6n-3 could involve heterotrophic protists such as dinoflagellates and ciliates grazing on small phytoplankton, as well as larger zooplankton such as copepods and salps, possibly feeding on microzooplankton and producing fecal pellets rich in 22:6n-3. According to LC-PUFA content, SPOM present throughout the upper water column (0–300 m) appeared of high nutritional quality both on- and off-plateau, and represented a valuable source of food for secondary consumers and suspension feeders.

Highlights

► FA profiles of SPOM from the Kerguelen region during the post-bloom period was dominantly composed of PUFA with high proportions of the two LC-PUFA 20:5n-3 and 22:6n-3. ► Abundance of LC-PUFA in the mixed layer derived from the phytoplankton community composed of small species (prymnesiophytes and prasinophytes) and diatoms. ► In the upper mesopelagic, LC-PUFA are maintained at high proportions according to distinct pathways, export of diatoms for 20:5n-3 and zooplankton fecal material for 22:6n-3. ► SPOM revealed high nutritional quality in the upper water column (0-300 m) both in the iron-fertilized area on the Plateau and outside in HNLC waters.

Keywords : Essential fatty acids, Vertical distribution, Fatty acid export, Phytoplankton diversity, Diatoms, Heterotrophic interactions, Nutritional quality

A. INTRODUCTION

The Southern Ocean (SO) is a vast and contrasted environment where the characteristics of pelagic ecosystems are particularly diverse. The Antarctic Circumpolar Current (ACC) composed of successive hydrographic fronts (Orsi et al., 1995) acts as a strong physical and biogeochemical boundary for biological activity, and to the south and until the Antarctic sea ice, lies the largest High Nutrient Low Chlorophyll (HNLC) zone of the world ocean. The productivity is low throughout the year in HNLC open waters essentially due to a lack of dissolved iron (Blain et al., 2007; de Baar et al., 1995; Martin, 1990), and high concentrations of unused macronutrients (phosphate, nitrate, silicic acid) persist in surface waters. In contrast, high productivity regimes are only found close or downstream of Subantarctic islands (South-Georgia, Crozet, Kerguelen, Heard) and continental shelves, which receive natural and persistent iron inputs (Blain et al., 2008; Perissinotto and Duncombe Rae, 1990; Pollard et al., 2007; van der Merwe et al., 2015; Venables and Moore, 2010). Iron fertilization allows phytoplankton, mainly initially composed of diatoms and also *Phaeocystis*, to thrive during intense and long-lasting blooms in austral spring/summer (Cavagna et al., 2015; Korb and Whitehouse, 2004; Mongin et al., 2008; Schallenberg et al., 2018; Schlosser et al., 2018; Seeyave et al., 2007). These blooms provide abundant food and energy to heterotrophic organisms and higher trophic levels, and help to maintain highly productive food webs extended from microbes to zooplankton, micronekton, up to emblematic top-predators of the SO (marine mammals, sea-birds, penguins, whales) (El-Sayed, 1988; Evans and Brussaard, 2012; Pakhomov and McQuaid, 1996).

In the current context of climate change, major modifications are predicted for the SO such as sea surface warming, increasing stratification and reduction in nutrient supplies, southward migration of oceanographic fronts, shrinking of sea ice, as well as ocean acidification, and it already concerns some areas like the Antarctic peninsula (Constable et al., 2014; Moline et al., 2004). These climate-induced changes are likely to affect phytoplankton distribution and composition (Deppeler and Davidson, 2017), and hence to have positive or negative cascade

effects on the whole food web. It is therefore important to determine what parameters control the present-day stability, health and resilience of these pristine ecosystems.

Among the parameters that maintains ecosystem stability, the nutritional value of phytoplankton is crucial, as it determines the amount of energy that can flow through the entire food web and controls its overall functioning. Part of nutritional quality for marine organisms is attributable to lipids, in particular to n-3 long-chain polyunsaturated fatty acids (n-3 LC-PUFA) such as 20:5n-3 (eicosapentaenoic acid, EPA) and 22:6n-3 (docosahexaenoic acid, DHA). n-3 LC-PUFA are molecules essential to all organisms and are involved in a variety of physiological processes such as growth, immunity, cell membrane function regulation and energy storage (Guschina and Harwood, 2006; Parrish, 2013). They play important roles in trophic interactions, starting from secondary consumers such as copepods and other crustacean zooplankton, for which they determine growth potential, reproduction success and general fitness (Brett et al., 2009; Brett and Müller-Navarra, 1997; Müller-Navarra et al., 2000; Pond et al., 2005). LC-PUFA are synthetized at the basis of the food web, essentially by phytoplankton and to some extent by small heterotrophs, and the supplies to consumers occur necessarily through diet (Bec et al., 2006; Guo et al., 2017; Klein-Breteler et al., 1999). The production of LC-PUFA by phytoplankton, and fatty acids (FA) in general, is highly species-specific both at the phylum and class levels (Cañavate, 2019; Jónasdóttir, 2019; Parrish, 2013) and enables their use as valuable biomarkers (Dalsgaard et al., 2003). Another consequence is that marine algae do not all have the same nutritional value, the most valuable algae in terms of LC-PUFA proportions includes Prymnesiophyceae, Pavlovaphyceae, Bacillariophyceae, Dinophyceae, Cryptophyceae, Eustigmatophyceae followed by, Prasinophyceae and Mamiellophyceae (Jónasdóttir, 2019). The lowest contents are found in Chlorophyceae, Trebouxiophyceae and especially in Cyanobacteria, which are devoid of LC-PUFA (Jónasdóttir, 2019).

In the SO, LC-PUFA are presumably supplied by two distinct groups of phytoplankton, diatoms and flagellates, characterized by specific FA profiles. Diatoms produce preferentially 20:5n-3 along with C16 monounsaturated fatty acids (MUFA) 16:1n-7, and C_{16} PUFA 16:3n-4 and 16:4n-1 (Dalsgaard et al., 2003; Parrish, 2013; Volkman et al., 1998), with only small amounts of

22:6n-3 found in centric diatoms (Dunstan et al., 1993). The other essential n-3 LC-PUFA 22:6n-3 together with C18 PUFA 18:5n-3 are produced preferentially by dinoflagellates as well as some Prymnesiophyceae like the coccolithophore *Emiliana huxleyi* (Jónasdóttir, 2019; Okuyama et al., 1992; Thomson et al., 2004) but this latter group is scarce in the SO, and thus it is not assumed to be a potential producer. Another important Prymnesiophyceae species, *Phaeocystis sp.*, produces low levels of LC-PUFA (Nichols et al., 1991; Skerratt et al., 1995), but it can represent an important part of the autotrophic biomass especially in the early and late phase of the diatom bloom. This general picture of LC-PUFA sources is generally adopted in diet studies and relies on the identification of diagnostic FA in consumers (Atkinson et al., 2006; Ericson et al., 2018; Hellessey et al., 2020). This generalized view is probably oversimplified as it mostly relies on FA signatures obtained from culture and feeding experiments without accounting for field observations. Moreover, it only takes into account a single autotrophic production pathway for LC-PUFA, whereas alternative routes via heterotrophy and upgrading may exist. As an example, interactions among grazers such as copepods and heterotrophic protozoans (dinoflagellates and ciliates) were shown to substantially increase the nutritional quality of *Phaeocystis globosa*, most probably via the production of LC-PUFA by heterotrophic upgrading (Tang et al., 2001).

For the SO, available data on the natural occurrence of LC-PUFA in phytoplankton, as well as in protists in general, remain scarce, and it received a disproportionally low attention in comparison to larger size organisms (Hellessey et al., 2020; Pond et al., 2005). The few available data concern only surface samples obtained from highly productive regions of the marginal ice zone and coastal Antarctic zone (Fahl and Kattner, 1993; Gillan et al., 1981; Hernando et al., 2018; Nichols et al., 1993; Thomson et al., 2004) as well as of the frontal Subantarctic zone of the Indian sector of the SO (Mayzaud et al., 2007, 2002). This clearly limits our understanding of LC-PUFA cycling in both the surface euphotic zone where production takes place, and in the water column where organic matter (OM) and associated LC-PUFA are considered as labile fraction, and could be degraded, transformed, and even transferred to benthic communities (Budge and Parrish, 1998; Rembauville et al., 2018; Wilson et al., 2010). Recent results obtained from five long-term sediment traps deployed in naturally iron-fertilized settings and HNLC waters of the Polar

Front (PF) region (South Georgia, Crozet, Kerguelen) indicate large regional and seasonal fluctuations in FA and PUFA composition of sinking OM (Rembauville et al., 2018). Variations are tightly linked to the ecological vectors responsible for the export of OM (e.g., diatom resting spores, phytoplankton aggregates, zooplankton fecal pellets) (Rembauville et al., 2016, 2015a, 2015b). On the Kerguelen Plateau, LC-PUFA such as 20:5n-3, which is usually associated to diatoms resting spores (mainly *Chaetoceros*), could be transferred at depth towards the sediments (Rembauville et al., 2018).

Among naturally Fe-fertilized regions, the Kerguelen Island area has received considerable interest over recent decades as it is well suited for studying the contrasted properties of pelagic ecosystems found in the SO. The Kerguelen Plateau, which extends to the southeast of the islands, is a large-scale topographic feature with shallow bathymetry (< 700 m) that benefits from enhanced Fe inputs via diapycnal mixing (Blain et al., 2008; Park et al., 2008) and is subjected to a large-scale (45,000 km²) and long lasting (October to February) diatom bloom (Mongin et al., 2008). Bloom phenology consists of two successive phases (Pellichero et al., 2020) with a first phase occurring in spring and dominated by small size diatoms forming long-chains (*Chaetoceros*, *Pseudo-nitzschia*) (Lasbleiz et al., 2016) and a second phase occurring in summer and dominated by larger size diatoms (*Eucampia*, *Corethron*) (Armand et al., 2008; Blain et al., 2021; Liu et al., 2020). Productivity is also stimulated downstream of the Plateau (according to the West to East ACC circulation) due to lateral advection of Fe-rich waters (Quéroué et al., 2015; Trull et al., 2015; van der Merwe et al., 2015), which promotes a diatom bloom from October to January. This latter bloom is shorter in duration and lower in intensity, and composed of different phytoplankton community composition in comparison to the central Plateau (Armand et al., 2008; Lasbleiz et al., 2016). Upstream of the Plateau, south-west of the Kerguelen Islands, open waters are away from the influence of the Fe fertilized area, productivity is drastically reduced and considered representative of HNLC conditions found in the SO (Rembauville et al., 2017). Phytoplankton biomass stays low throughout the year (climatological Chlorophyll a (Chl-a) < 0.3 $\mu g.L^{-1}$) except during a short time period (~1 month) in December/January (Fiala et al., 1998; Kopczyńska et al., 1998). Under HNLC regime, pico- and nano- communities composed mostly by *Phaeocystis sp.* predominate most of the time, except during summer when

microphytoplankton, such as small diatoms (*Fragilariopsis sp.*) and autotrophic dinoflagellates, are more abundant (Armand et al., 2008; Fiala et al., 1998; Kopczyńska et al., 1998; Lasbleiz et al., 2016; Rembauville et al., 2017).

The MOBYDICK project (Marine Ecosystem Biodiversity and Dynamics of Carbon around Kerguelen: an integrated view) was designed to complement the available description of the Kerguelen region ecosystems and the main objectives were 1) to track carbon from its initial fixation at the surface to its channeling through the food web and its transfer at depth via export, and 2) to perform a detailed description of the diversity at each trophic level. The oceanographic survey was carried out in late summer/early autumn (February-March 2018) corresponding to the demise of the diatom bloom, a period that was not previously investigated by other surveys carried out during the onset (KEOPS2, October-November 2011) and decline (KEOPS1, January-February 2005) of the bloom. In this study, we investigated the distribution of FA, including the essential LC-PUFA 20:5n-3 and 22:6n-3, in suspended organic matter (SPOM) collected in the upper water column. Our aims were to explore the origin and fate of essential LC-PUFA from the surface to the upper mesopelagic zone at sites with contrasted seasonal productivity regimes found on and off the Kerguelen Plateau. Statistical analyses were used to identify the main drivers of FA profile variability. A selection of FA specific to phytoplankton classes and zooplankton activity was used to identify the main producers of LC-PUFA and to explore the impact of heterotrophic interactions in the upper water column. Finally, PUFA contents were used to discuss the nutritional quality of suspended OM and a comparison between iron-fertilized and HNLC conditions was addressed.

B. MATERIAL & METHODS

Studied area

The MOBYDICK survey was conducted in the Kerguelen Islands area in the Indian sector of the SO on board of *R/V Marion Dufresne II* during late-austral summer 2018 from February 18th to March 28th coinciding with the post bloom phase. Four stations (M1, M2, M3, and M4, Figure 1), were selected to represent the contrasted production regimes encountered in the area and defined on a seasonal basis. Station M2 (bottom depth 520 m) is located in the Fe-enriched area

on the central Kerguelen Plateau. This station corresponds to the station A3 investigated during KEOPS1 and KEOPS2 programs. Station M1 (bottom depth 2723 m), located downstream of the Plateau, benefits also from enhanced Fe supplies and exhibit a seasonal moderate production regime. Station M3 (bottom depth 1730 m) and M4 (bottom depth 4731 m) are both located upstream of the Plateau and are representative of HNLC conditions. Station M3, previously investigated as part of the KERFIX time series program (1990-1995) (Jeandel et al., 1998), was at the time of sampling north of the PF in the Polar Frontal Zone (PFZ) according to Pauthenet et al. (2018), while the three other stations were permanently south of the PF. During the survey, repeated visits were performed at most stations at around 10-day interval except at station M1, which was visited only once. As shown in Table 1, three visits were performed at station M2 (M2-1, M2-2, and M2-3) and two at stations M3 and M4 (M3-1, M3-3, M4-1, M4-2).

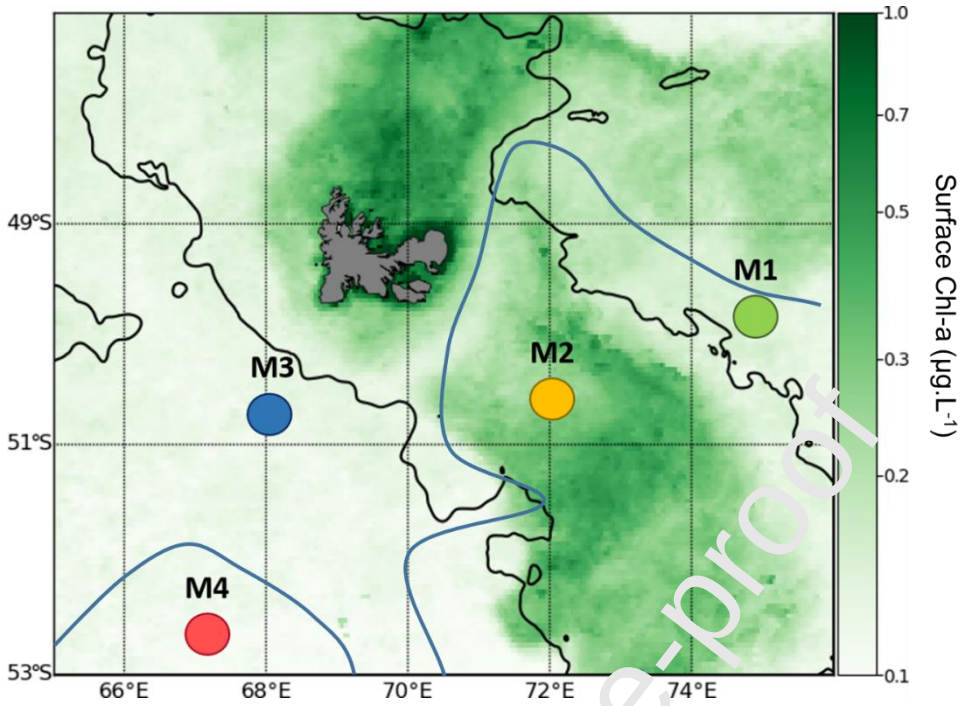

Figure 1 Map of MOBYDICK station locations and monthly mean (March 2018) surface Chlorophyll-a concentrations (µg.L^{-1}) obtained from 4 km resolution Global Ocean Satellite Observations (Copernicus-Globcolour, Copernicus Marine Service, http://marine.copernicus.eu/). The black line refers to 1000 m bathymetry and the blue refers to the approximate position of the PF for the Feb.-Mar. period and drawn according to Pauthenet et al. (2018).

Hydrological and biogeochemical data

Vertical profiles of temperature, dissolved oxygen, and salinity were obtained at all stations using a SeaBird 911-plus CTD (Conductivity, Temperature, and Density) unit mounted on the rosette. Chl-a concentrations and PAR (photosynthetically available radiation) levels were measured using a fluorometer and LI-COR sensor, respectively. The mean depth of the mixed layer (MLD) was estimated based on a difference in potential density of 0.03 to the surface value (10 m) and using all CTD casts performed during the occupation of stations (Lafond et al., 2020). The depth of the euphotic zone (Z_e) corresponded to the depth where light intensity was at least 1% of incident light at the surface (Table 1). Averaged Chl-a, silicic acid ($Si(OH)_4$) and ammonium (NH_4^+) concentrations for the mixed layer (ML) are also shown in Table 1, details on the analytical methods can be found elsewhere (Irion et al., 2020; Lafond et al., 2020).

Table 1. MOBYDICK station details, averaged depth of the mixed layer (MLD), depth of the euphotic zone (Ze), and averaged concentrations of Chl-a, silicic acid, ammonium in the mixed layer.

Station	Lat	Lon	Bottom depth	date	Visit	MLD[a]	Ze[b]	Chl-a		$Si(OH)_4$		NH_4	
	°S	°E	m			m	m	µg.L^{-1}		µmol.L^{-1}		µmol.L^{-1}	
								Mean	S.D	Mean	S.D	Mean	S.D
M1	49.9	74.9	2723	10/03/2018	M1	63	89	0.34	0.04	6.7	0.3	0.57	0.21
M2	50.6	72.0	520	27/02/2018	M2-1	79	64	0.27	0.02	1.4	0.4	0.75	0.08
				06/03/2018	M2-2	73	61	0.31	0.05	1.7	0.8	1.12	0.03
				12/03/2018	M2-3	80	58	0.59	0.03	2.8	0.3	0.95	0.06
M3	50.7	68.1	1730	05/03/2018	M3-1	74	93	0.21	0.03	2.9	1.0	0.63	0.22
				19/03/2018	M3-3	96	105	0.14	0.00	2.3	0.2	0.73	0.01
M4	52.6	67.2	4731	03/03/2018	M4-1	69	95	0.19	0.01	4.4	0.4	0.37	0.03
				14/03/2018	M4-2	96	101	0.21	0.01	5.3	1.0	0.54	0.11

[a] MLD: Average mixed layer depth estimated from multiple CTD casts at each station and according to potential density fluctuations < 0.03 kg.m^{-3} relative to 10 m depth.

[b] Ze: Depth of the euphotic zone defined as 1% of surface photosynthetic active radiation.

Sampling of suspended particles

Suspended particulate organic matter (SPOM) was sampled for FA determination, at all visited stations (8 stations in total) using five *in situ* pumping systems (ISP) allowing large volume of seawater to be filtered (200-1500 L) and sufficient amount of material to be collected. The five ISP were deployed from the surface euphotic zone to the upper mesopelagic, down to

200 m (M1, M2-2, M2-3, M4-2), 300 m (M2-1, M3-1, M3-3), and 600 m depth (M4-1). For three stations (M1, M2-1, M4-1), only four depths could be sampled due to ISP failures. ISP were equipped for sequential filtration, and we considered here only the 1-50 μm size fraction, which corresponds to the largely dominant fraction in terms of Particulate Organic Carbon (POC, averaged weight proportion 93% of total POC, n=37). For the first six stations (M1, M2-1, M2-2, M4-1, M4-2, M3-1), the 1-50 μm size fraction was obtained from a single filter made of high-purity quartz microfiber (QMA, Sartorius, France) of 1 μm nominal pore size, and placed after two successive nylon (NITEX) screen pre-filters of 300 and 50 μm mesh size. For the last two stations (M2-3 and M3-3), due to a change in the mesh size of screens (50 and 20 μm), the 1-50 μm fraction was obtained from the QMA filter (1-20 μm) and from the intermediate screen of 20 μm mesh size (20-50 μm).

Samples processing on board

After ISP recovery, the QMA filters were processed on-board as follows: subsampling was conducted directly on the filter using a 25 mm plexiglass punch previously cleaned with ethanol. For FA analyses, four punches were taken and then extracted in 6 mL of 2:1 (v:v) chloroform:methanol solvent and preserved at -20°C. For POC measurements, four other punches were taken, dried at 55°C for 24 hours, and stored at room temperature. For the NITEX screens, the 142 mm filters were cut into quarters using a scalpel (ethanol cleaned), and one quarter was dedicated to POC analyses and another to FA analyses. The two remaining quarters were kept as spare at -20°C. Particles from the NITEX were resuspended using filtered seawater (0.4 μm) and recollected on a pre-combusted 0.7 μm nominal pore-size glass fiber filters (Whatman GF/F, Maidstone, UK). The GF/F filters were processed as described for QMA filters for FA (dived in 6 mL of chloroform:methanol solvent and stored at -20°C) and POC analyses. Lipid extracts dedicated to FA analyses were stored at -20°C during the cruise, shipped to home laboratory (France) with dry ice and stored at -20°C until FA analyses.

Particulate organic carbon analyses

POC samples were fumed with hydrochloric acid (10M) for 4 hours to remove particulate inorganic carbon, dried at ambient temperature for 2 hours, subsampled with a 13 mm punch

and encapsulated into tin caps following protocols by Brook et al. (2003) and Trull et al. (2015). POC content was determined using a Flash Elemental Analyzer 2000 coupled to a Thermo Fisher Delta V Plus stable light isotope ratio mass spectrometer system (IRMS, Bremen, Germany). Data were corrected for filter blank contribution, and acetanilide (C_8H_9NO) was used as a standard for POC content. Final concentrations of POC in seawater are reported in $\mu mol.L^{-1}$.

Fatty acids analysis

a. Lipid extraction and purification

Samples for FA analyses were re-extracted to remove any residual seawater. The initial lipid extract was transferred in a new 22 mL vial, and then re-extracted with 3 mL of chloroform. The sample was vigorously shaken and then centrifuged to insure a good phase separation. For each sample, three re-extractions were performed. Lipid extracts were then evaporated with N_2 gas, resuspended in 6 mL of chloroform:methanol (2:1 v:v) and stored at -20°C until analysis. Lipid extracts were separated into neutral and polar lipids following the method of Remize et al.(2020). Briefly, 3 mL of total lipid extract was evaporated with nitrogen, recovered with three washes using chloroform:methanol (final volume 1.5 mL, 98:2 v:v) and spotted at the top of a silica gel column (40 mm ×4 mm, silica gel 60A 63–200 μm rehydrated with 6% H_2O, 70–230 mesh, Sigma-Aldrich, Darmstadt, Germany). The neutral lipid fraction (NL) was eluted using chloroform:methanol (10 mL, 98:2 v:v) and the polar lipid fraction (PL) with methanol (20 mL). Both fractions were then collected in glass vials, and an internal standard (C23:0, 2.3 μg) was added.

b. Transesterification of FAME

Fatty acids methyl esters (FAME) transesterification was conducted according to the protocol described by Mathieu-Resuge et al. (2019). In brief, after evaporation to dryness of the NL and LP fractions, transesterification was performed by adding 0.8 mL of H_2SO_4/methanol mixture (3.4% v:v) to the lipid extract and heated at 100 °C for 10 min. Hexane (0.8 mL) and distilled water saturated with hexane (1.5 mL) were added. The lower MeOH–water phase was

discarded after homogenization and centrifugation. Hexane fraction containing FAME was washed two more times with another 1.5 mL of distilled water.

c. Fatty acid analysis by gas chromatography

Analyses of FAME were performed on a Varian CP8400 gas chromatograph (Agilent, Santa Clara CA, USA) using simultaneously two separations on a polar column (ZBWAX: 30 mm × 0.25 mm ID × 0.2 µm, Phenomenex, Torrance, CA, USA) and an apolar column (ZB5HT: 30 m × 0.25 mm ID × 0.2 µm, Phenomenex, Torrance, CA, USA). The temperature program used by the gas chromatograph was the following: first, initial heating to 0 from 150 °C at 50 °C.min^{-1}, then to 170 °C at 3.5 °C.min^{-1}, to 185 °C at 1.5 °C.min^{-1}, to 225 at 2.4 °C.min^{-1} and finally to 250 °C at 5.5 °C.min^{-1} and maintained for 15 min. The FAME were identified by comparison of their retention time with commercial and in-house standards mixtures as described in Remize et al. (2020).

Table 2. Complete list of FA determined in this study and grouped by compound family with saturated fatty acids (SAFA), monounsaturated fatty acids (MUFA), polyunsaturated fatty acids (PUFA), and branched fatty acids (Branched). Major FA (> 1% of TFA of the mean of all samples) are highlighted in bold.

Group	Fatty acids
SAFA	**14:0**, 15:0, **16:0**, 17:0, **18:0**, 20:0, 21:0, 22:0, 24:0
MUFA	14:1n-5, 15:1n-5, 16:1n-9, **16:1n-7**, 16:1n-5, 17:1n-7, **18:1n-9**, **18:1n-7**, 18:1n-5, 20:1n-9, 20:1n-7, 22:1n-9, 22:1n-7, 24:1n-9
PUFA	C_{16}: 16:2n-7, 16:2n-6, 16:2n-4, 16:3n-4, 16:3n-6, 16:3n-3, 16:4n-3, **16:4n-1**
	C_{18}: **18:2n-6**, 18:2n-4, 18:3n-6, 18:3n-4, **18:3n-3**, 18:4n-1, **18:4n-3**, **18:5n-3**
	C_{20}: 20:2n-6, 20:3n-6, 20:3n-3, 20:4n-6, 20:4n-3, **20:5n-3**
	C_{21}: 21:5n-3
	C_{22}: 22:2n-6, 22:4n-6, 22:5n-6, 22:5n-3, **22:6n-3**
Branched	iso15:0, ante15:0, iso16:0, iso17:0

FA concentrations reported here correspond to the total lipid fraction (sum of PL and NL fractions) measured in 1-50 μm SPOM. Concentrations are reported in $\mu g.L^{-1}$ (of seawater) as well as in percent mass proportion relative to total fatty acids (%TFA). The complete list of FA considered and grouped by compound family is shown in Table 2. FA are reported using a shorthand notation of A:Bn-x, where A indicates the number of carbon atoms, B is the number of double bonds and x indicates the position of the first double bond relative to the terminal methyl group (Budge et al., 2006).

Fatty acid profiles in phytoplankton classes

In Table S1, we summarized available information on FA composition of phytoplankton classes provided by the meta-analysis of Jónasdóttir (2019) and Cañavate (2019) as well as the screening study of Mitani et al. (2017). This allows to highlight the relationships between some specific FA abundances and phytoplankton classes.

As seen in Table S1, the percentage of 14:0 is usually above 10% in Mamiellophycea (MAM), Pavlovophycea (PAV), Pelagophycea (PEL), Cosciondiscophycea (COS) and Mediophycea (MED) and above 15% in Coccolithophycea (COC), Prymnesiophycea (PRY), Pinguiophycea (PIN) and Fragilariophycea (FRA). The percentage of 16:1n-7 is above 15% in PAV, Bacillariophyceae (BAC), COS, FRA, and MED. The sum of 16:2n-7, 16:2n-4, 16:3n-4 and 16:4n-1 account for 12% in BAC, 21% in COS, 12% in FRA and 19% in MED while they are only present in trace amounts in other phytoplankton classes. The percentage of 16:4n-3 is above 10% in Chlorophyceae (CHL), Chlorodendrophyceae (CHD), Pyramimonadophyceae (PYR), Prasinophyceae (PRA) and MAM. Percentage of 18:2n-6 is present at 11% in Cyanophyceae (CYA) and 14.5% in Trebouxiophyceae (TRE) while 18:3n-6 is only above 5% in CYA. 18:3n-3 and 18:4n-3 are present in most phytoplankton classes; 18:3n-3 is above 15% in CYA, CHL, TRE, CHD, and Cryptophycea (CRY) while 18:4n-3 is above 12% in PYR, PRA, MAM, CRY PRY, Raphydophyceae (RAP), and PEL. The percentage of 18:5n-3 is especially high in Dinophyceae (DIN) (16%) and present above 5% in PYR, PRA, COC, and PRY. The percentage of 16:4n-3 is above 12% in CHL, CHD, PYR, PRA and MAM, all belonging to the chlorophyta phylum. 20:5n-3 (EPA) ranged between 15% and 20% in PAV, RAP, BAC, COS, FRA, and MED and above 20%

in Porphyridophyceae and PIN. 22:6n-3 (DHA) is above 10% in COC, and PRY and above 15% in DIN.

Fatty acids associated to heterotrophic organisms

Branched FA (iso15:0, anteiso15:0, iso16:0 and iso17:0) are associated to bacteria (Parrish, 2013; Volkman et al., 1998; Wilson et al., 2010). The MUFA 20:1n-9, 22:1n-9, 22:1n-7 and 22:1n-11 are specifically produced by zooplankton such as Calanoids (Brett et al., 2009; Dalsgaard et al., 2003; Kattner and Hagen, 1995; Mayzaud et al., 2007; Parrish, 2013; Wilson et al., 2010) and are not found in phytoplankton.

FA-based nutritional quality index

FA data were used to estimate the nutritional quality of the 1-50 µm SPOM following the FA-based nutritional quality index (NQI) developed by Cañavate (2019). The NQI was calculated as follow:

$$\mathrm{NQI} = [(15 * \mathrm{DHA} + 10 * \mathrm{EPA} + 2 * \mathrm{ARA}) * 0.8 + (1.8 * \sum \mathrm{C18PUFA})] * \log\left(\frac{n-3}{n-6}\right)$$

DHA, EPA and 20:4n-6 (arachidonic acid, ARA) are expressed as % of TFA. ΣC18PUFA is the sum of 18:2n-6, 18:3n-3, 18:4n-3 and 18:5n-3 percentages and n-3/n-6 is the ratio of total n-3 PUFA to total n-6 PUFA.

Statistical analysis

Principal Component Analysis (PCA) was used to characterize relationships among FA and to discriminate FA profiles according to depth and station. The PCA was performed with 36 FA out of 55 analyzed whose average abundance was >0.1% of TFA. Resulting components 1, 2 and 3 were analyzed using one-way analysis of variance (ANOVA) to identify differences of FA profiles according to depth intervals (ML, MLD-150 m, 150-300 m) and stations. Categories of branched FA, SAFA, MUFA, short-chain PUFA (SC-PUFA), and LC-PUFA were analyzed by non-parametric one-way ANOVA (Krustal-Wallis) with post-hoc analysis to determine significant differences between depth zones (ML, MLD-150 m, 150-300 m). Furthermore, spearman tests were conducted to explore the relationship between some FA and depth. In the

surface mixed layer (ML), FA profiles of the 1-50 μm fraction were analyzed by non-parametric one-way ANOVA (Krustal-Wallis) with post-hoc analysis to determine significant differences among stations. Spearman tests were also conducted to explore the relationship between FA profiles and physico-chemical parameters (Temperature, Salinity, Oxygen, NH_4^+, $Si(OH)_4$, NO_3^-) in the ML. Differences were considered statistically significant if $p<0.05$. All statistical analyses were performed using Statgraphics Plus statistical software (Manugistics, Rockville, MD, USA).

C. RESULTS

Hydrological and biogeochemical context

During the first half of the MOBYDICK survey, from late February to early March, the MLD was relatively shallow at all stations (Table 1), varying from 63 m at station M1 to 79 m at station M2-1, and it was consistent with late summer conditions (stable upper water column and low wind stress). After a storm event that occurred on the 10th of March, the MLD deepened consistently at stations M4-2 and M3-3 reaching 96 m, and to a lesser extent on the Plateau at station M2-3 (80 m). The depth of Ze was shallow on the plateau (58-64 m) and above the MLD. Ze was deeper at the other stations (89 m at M1 down to 105 m at M3-3) and it was below the MLD indicating no light limitation in the ML.

In the ML, Chl-a exhibited low values at all stations, with 0.27-0.59 $\mu g.L^{-1}$ and 0.14-0.34 $\mu g.L^{-1}$ on- and off-plateau, respectively. At station M2, Chl-a almost doubled between the second (M2-2) and the third visit (M2-3). Silicic acid had variable concentrations in the ML (Table 1). These were the lowest on the plateau at M2-1 and M2-2 (1.4-1.7 μM), intermediate at M3 (2.3-2.9 μM) and the highest at M4 (4.8 μM) and M1 (6.7 μM). As a comparison, ammonium concentrations, an indicator of heterotrophic excretion, exhibited a reverse trend with highest values on the plateau (0.7-1.1 μM) decreasing to 0.6-0.7 μM at M3 and M1, and were the lowest at M4 (0.3-0.5 μM).

Vertical distribution of TFA concentrations

Depth weighted average (DWA) of TFA concentrations obtained for three depth intervals (ML, MLD-150 m, 150-300 m) are shown in Figure 2. Considering all stations and visits, TFA

concentrations were significantly ($p<0.001$) higher in the ML (range: 1.4-3.6 $\mu g.L^{-1}$) as compared to the deeper zones (MLD-150 m and 150-300 m). Although TFA concentrations tended to be lower in the 150-300 m depth interval (range: 0.2-0.7 $\mu g.L^{-1}$) compared to the MLD-150 m zone (range: 0.6-1.6 $\mu g.L^{-1}$), the difference was not significant. TFA concentrations were significantly related to POC ($R^2=0.91$ and $p<0.001$, n=24) and therefore to biomass variability. Based on the slope of the regression, the average concentration of TFA in biomass was estimated to be 79±5 $\mu g.mgC^{-1}$.

In the ML, TFA concentrations were not significantly ($p>0.05$) different between on- and off-Plateau stations despite different temporal trends. On the Plateau, TFA concentrations increased from 1.7 to 2.9 $\mu g.L^{-1}$ between stations M2-1 and M2-3. Off the Plateau, TFA concentrations decreased during the course of the survey, from 2.3 to 1.5 $\mu g.L^{-1}$ at station M3 and from 2.4 to 1.4 $\mu g.L^{-1}$ at station M4. The highest TFA concentration in the ML (3.6 $\mu g.L^{-1}$) was found at station M1 downstream of the Plateau. Below the ML, no significant differences ($p>0.05$) were observed according to station locations. On the Plateau, TFA concentration was higher during the first visit of M2-1 (1.6 $\mu g.L^{-1}$) decreasing to 0.6 $\mu g.L^{-1}$ at M2-2, ten days later.

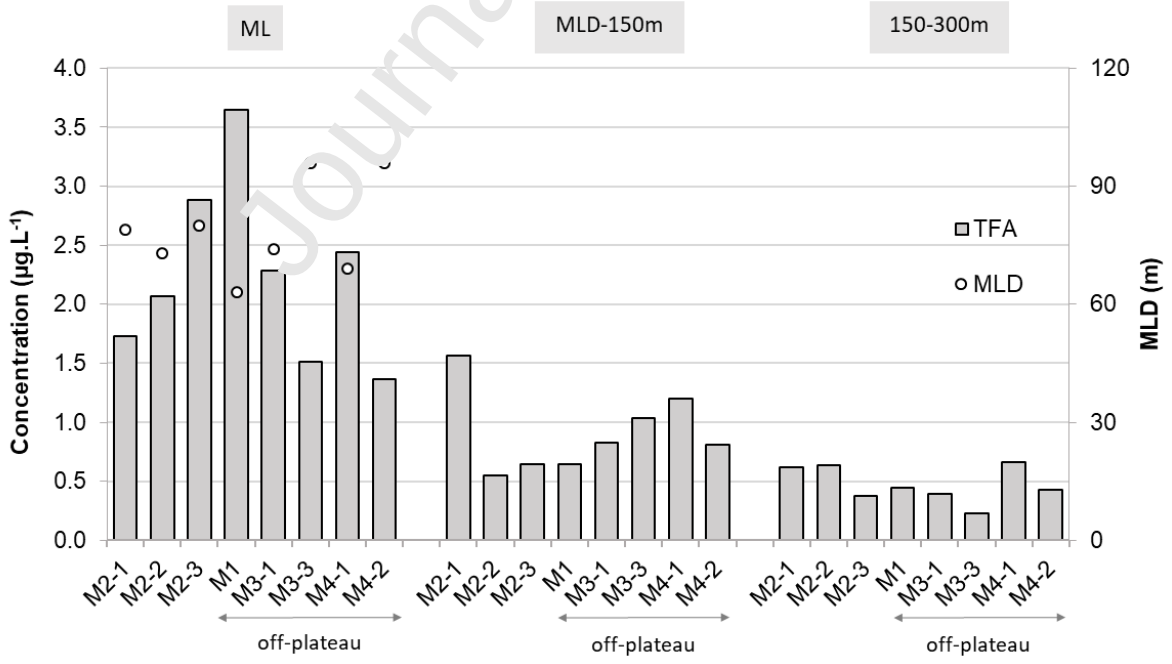

Figure 2: Depth weighted average TFA concentrations (µg.L-1) obtained in three depth intervals (ML, MLD-150m, 150-300m) according the station-visit sampled during the cruise. Also shown, the MLD (m) which was estimated for all stations.

FA partitioning according to unsaturation level

A preliminary partitioning of FA was performed according to the unsaturation level as described in Table 2 and considering branched FA, SAFA, MUFA and PUFA. Within PUFA, we

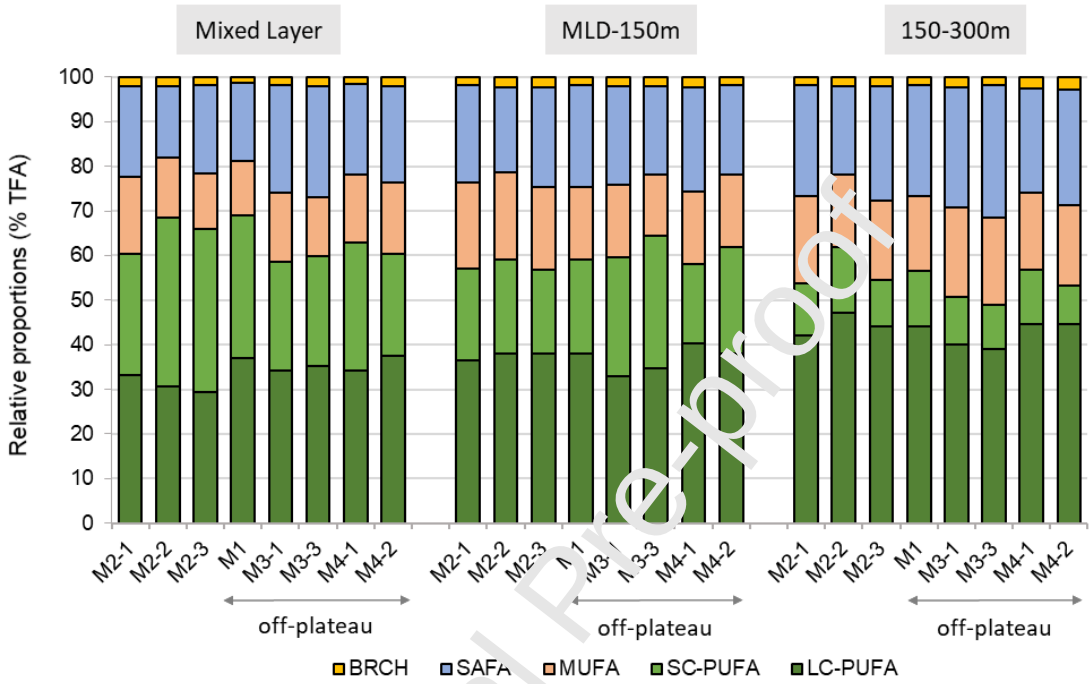

Figure 3: Depth-weighted averaged percentages (relative to TFA) of branched FA (BRCH), saturated FA (SAFA), monounsaturated FA (MUFA), short-chain (C16-C18) and long-chain (C20-C22) polyunsaturated FA (SC-PUFA and LC-PUFA) in three depth intervals (ML, MLD-150, 150-300m).

further distinguished SC PUFA with 16 and 18 atoms of carbon from long-chain PUFA (LC-PUFA) containing 20 and 22 atoms of carbon, which included the essential 20:5n-3 and 22:6n-3. Depth weighted average percentages (relative to TFA) of these five groups are shown in Figure 3. Considering all stations and depths, PUFA were the predominant category (62% on average), followed by SAFA (21% on average), MUFA (15% on average), and Branched FA (2% on average). Within PUFA, LC-PUFA were dominant (range: 34-44%) and showed increasing and significantly different ($p<0.001$) proportions according to depth interval, 34% in the ML, 37% in the MLD-150 m, and 45% in the 150-300 m. On the opposite, SC-PUFA decreased substantially with depth, from 30% in the ML down to 12% in the 150-300 m depth interval, and differences between all depth intervals were significant ($p<0.001$). For SAFA and MUFA, proportions

increased with depth. Differences were significant ($p<0.01$) only in the 150-300 m compared to the ML and MLD-150 m for SAFA, and in the ML compared to the MLD-150 m and 150-300 m for MUFA.

In the ML, no significant differences were observed for SAFA, MUFA, and Branched between on- and off-plateau. LC-PUFA tended to be higher off-plateau compared to on-plateau while SC-PUFA tended to be higher on the plateau vs off-plateau. Below the ML, no significant differences were observed among stations. However, the decrease of SC-PUFA with depth was faster on the plateau (from 34 to 20%) as compared to off-plateau (from 28 to 24%).

LC-PUFA were dominated by 20:5n-3 and 22:6n-3, both increasing significantly with depth from 13% to 19% for 20:5n-3 and from 18% to 20% for 22:6n-3. SC-PUFA decreased significantly with depth due to the decreases of 18:3n-3, 18:4n-3 and 18:5n-3. In contrast, C16 PUFA associated to diatoms were significantly higher in deep zones (MLD-150m and 150m-300m divisions) than in the ML.

Overall pattern in individual FA abundance

Principal component analysis was applied to 36 FA relative abundances (expressed as % of TFA) by examining 37 cases including FA compositions from 8 stations at various depths and visits. As shown in Figure 4, axis 1 and 2 explained 34.1% and 17.1% of the variability, respectively, and axis 3 12.3% (not shown in Fig. 4). These three axis accounted for >63% of total variability. The positive side of axis 1 was driven by 15:0, 16:0, 18:1n-7, 20:1n-9, 22:1n-9, and 22:1n-7 while 17:1n-7, 18:2n-6, 18:3n-6, 18:3n-3, 18:4n-3 and 18:5n-3 were correlated with the negative side of axis 1. The second axis of the PCA was positively associated to diatom markers including 16:2n-7, 16:2n-4, 16:3n-4, 16:4n-1 and 20:5n-3 and negatively associated to 18:1n-9. The third axis was positively correlated to 16:4n-3. All correlations previously listed (positive or negative) between FA variables and principal components 1, 2, and 3 were highly significant and had correlation coefficients greater than 0.7. As PC1, PC2, and PC3 revealed good correlations (positive and negative) between FA variables, non-parametric analyses of variance with PC1, PC2, and PC3 as the dependent variables and depth intervals and stations as the independent variables were performed. The analysis showed that differences in FA profiles

attributable to depth were highly significant (Figure 5) for both PC1 and 2 with p values <0.001 in both cases. While PC1 value increased steadily with depth zones, PC2 value of the MLD-150 m was higher than in the ML and 150-300m zones. While PC1 and PC2 were not significantly different according to stations, PC3 allowed significant differentiation between on-plateau station M2 and off-plateau stations M3 and M4 ($p<0.01$, Figure 5).

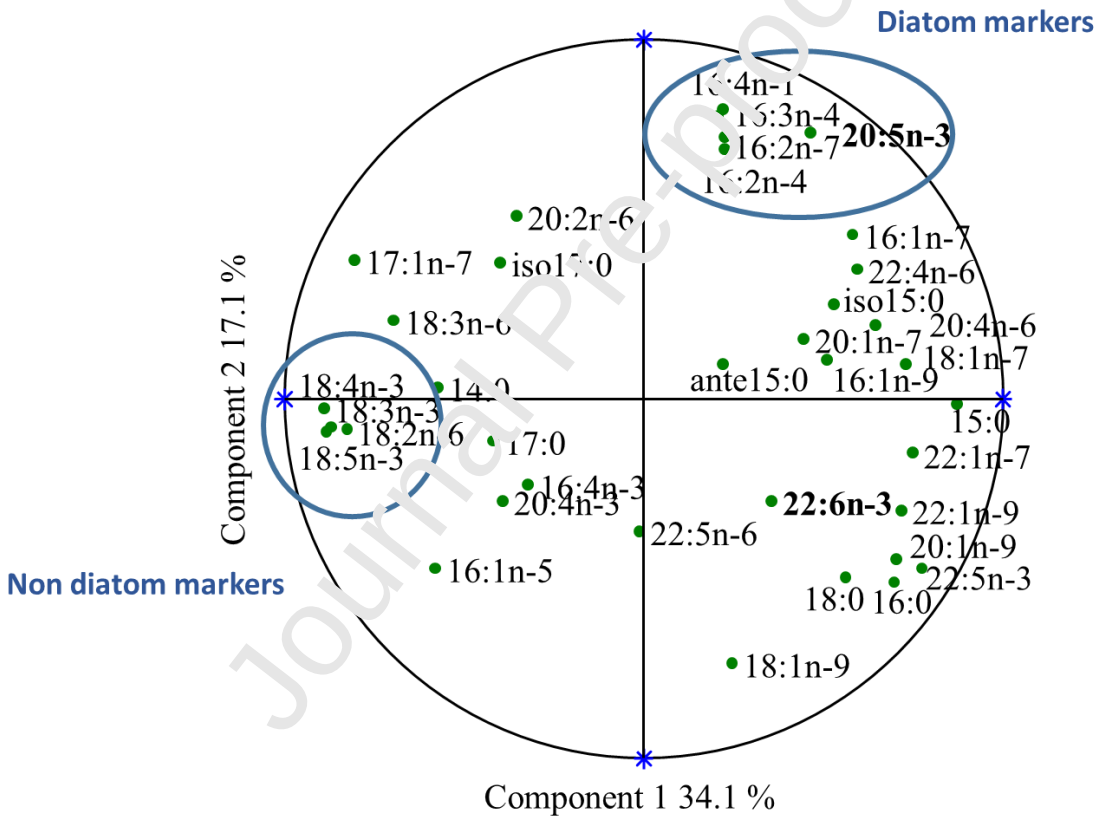

Figure 4: Correlation circle of 36 fatty acid variables according to the two principal components 1 and 2 obtained from the Principal Component Analysis, which used 37 cases including FA compositions of 1-50 µm suspended particulate organic matter from 8 stations at various depths. The outer circle represents the unit circle in terms of correlation coefficient (positive or negative along each axis). The closer the FA variables are to the outer circle, the higher the correlation coefficient.

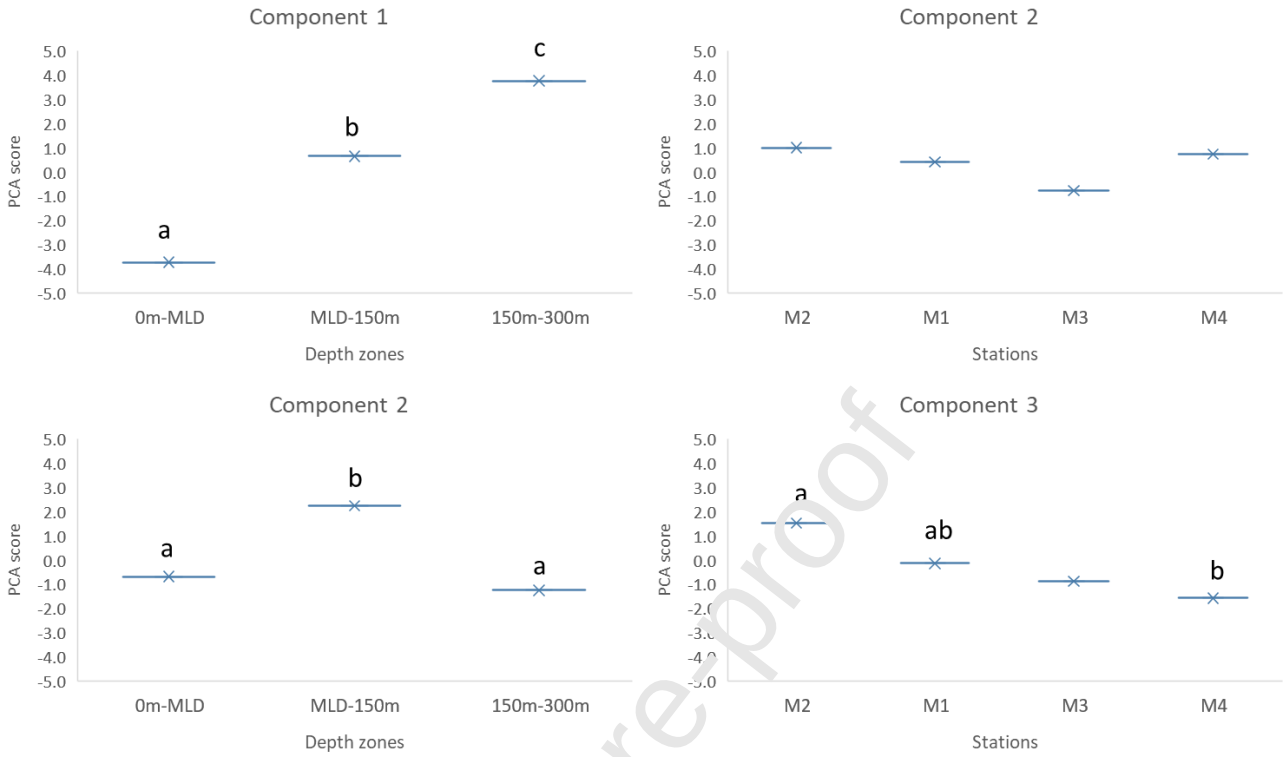

Figure 5: (Left) Non-parametric analysis of variance with PC1 and PC2 as the dependent variables (all stations pooled) and depth intervals as the independent variable; (Right) Non-parametric analysis of variance with PC2 and PC3 as the dependent variables (all depth intervals pooled) and stations as the independent variable. Letters a, b and c indicate statistical differences among conditions.

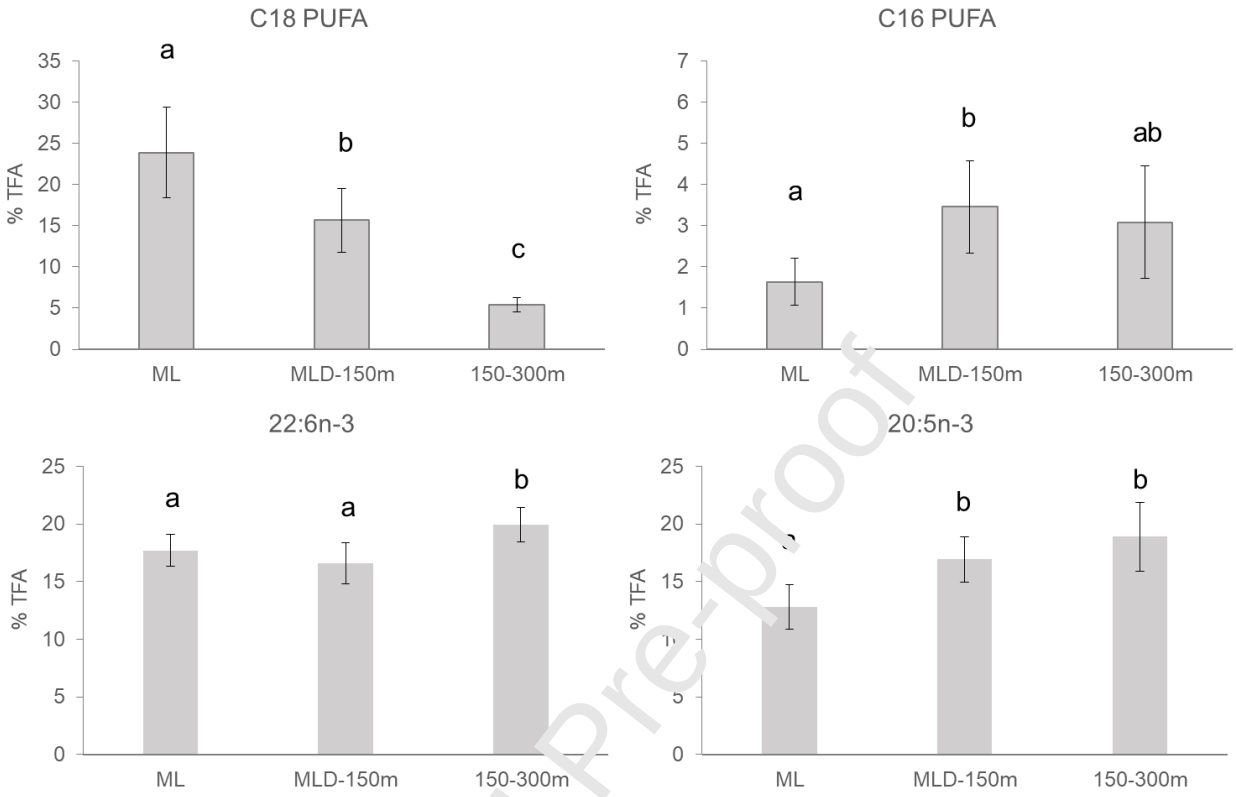

Figure 6: Percentages (relative to TFA) of C18 PUFA (sum of 18:3n-3, 18:4n-3 and 18:5n-3), C16 PUFA (sum of 16:2n-7, 16:2n-4, 16:3n-4 and 16:4n-1), 22:6n-3 and 20:5n-3 according to depth intervals. Letters a, b and c indicate statistical differences among conditions.

FA variability according to depth and stations

Furthermore, we explored the relationships between proportions of individual FA and depth (considering all stations together). Depth explained significantly the variability of 17:1n-7 (R^2=61%, p<0.0001), 18:2n-6 (R^2=30%, p<0.001), 18:3n-6 (R^2=37%, p<0.001), 18:3n-3 (R^2=44%, p<0.0001), 18:4n-3 (R^2=49%, p<0.0001), 18:5n-3 (R^2=44.7%, p<0.0001) through negative linear regressions. R^2 values were improved using Log regression for 18:2n-6 (R^2=50%, p<0.0001), 18:3n-3 (R^2=61%, p<0.0001), 18:4n-3 (R^2=68%, p<0.0001), 18:5n-3 (R^2=68%, p<0.0001). At the opposite, depth explained significantly the variability of 16:0 (R^2=68%, p<0.0001), 18:1n-9 (R^2=56%, p<0.001), 20:1n-9 (R^2=78%, p<0.0001), 22:1n-7 (R^2=41%, p<0.0001), 22:1n-9 (R^2=36%, p<0.001), and 22:5n-3 (R^2=79%, p<0.0001), through positive linear regressions. The best fitting regressions for 18:4n-3, 18:5n-3, 20:1n-9 and 22:5n-3 as a function of depth are presented in

Figure S1. Variations according to depth concerned also LC-PUFA 20:5n-3 and 22:6n-3, and diatom C16 PUFA (the sum of 16:2n-7, 16:2n-4, 16:3n-4 and 16:4n-1) as illustrated in Figure 6 for the three depth intervals considered. Averaged proportions of 20:5n-3 and diatom C16 PUFA were significantly higher in the MLD-150m and 150-300m depth intervals in comparison to the ML. For 22:6n-3, relative proportions remained high throughout the upper water column (0-300m) ranging from 18 to 20% of TFA, and were significantly higher in the deepest depth zone (150-300m).

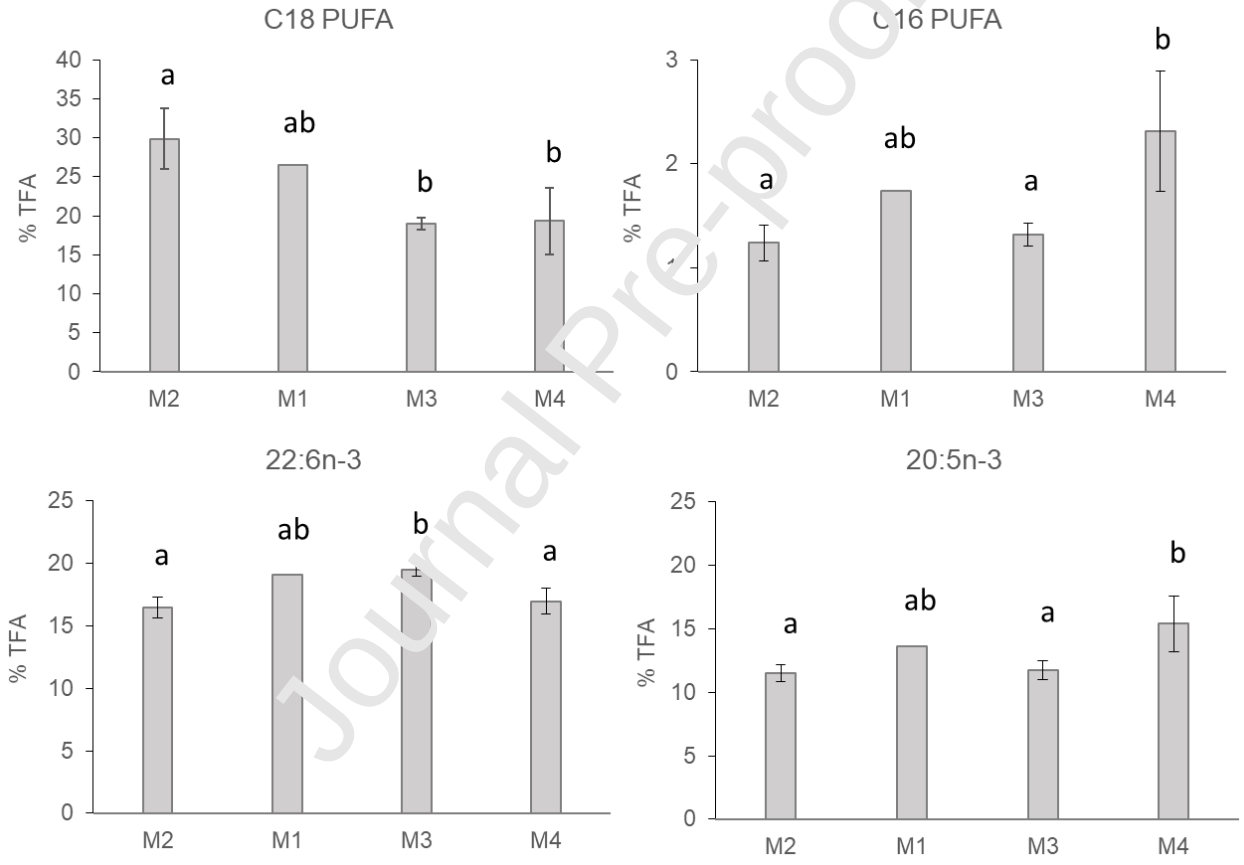

Figure 7: Percentages (relative to TFA) of C18 PUFA (sum of 18:3n-3, 18:4n-3 and 18:5n-3), C16 PUFA (sum of 16:2n-7, 16:2n-4, 16:3n-4 and 16:4n-1), 22:6n-3 and 20:5n-3 according to stations in the ML. Letters a and b indicate statistical differences among conditions.

Considering the significant differences between depth intervals, we compared FA profiles among stations within depth zones (Figure 7 for the ML). In the ML, the sum of 18:3n-3, 18:4n-3 and 18:5n-3 proportions was significantly higher at M1 and M2 stations compared to M3 and M4

stations off the plateau. The sum of diatoms C16 PUFA (16:2n-7, 16:2n-4, 16:3n-4 and 16:4n-1) and the proportion of 20:5n-3 were significantly higher at station M4 than at stations M2 and M3. No difference among stations were found within both MLD-150m and 150m-300m zones.

To attempt explaining difference of FA composition among stations, relationships between physico-chemical parameters and FA composition were explored. We only considered regressions with $R^2 > 40\%$ with p value <0.01. Diatoms C16 PUFA and 20:5n-3 proportions were statistically negatively correlated to temperature (R^2=47% and 44%, respectively, with p <0.01, Figure S2). The sum of 18:3n-3, 18:4n-3 and 18:5n-3 was positively correlated to NH_4^+ (R^2=41%, p<0.01, Figure S2).

Diatom C16 PUFA and 20:5n-3

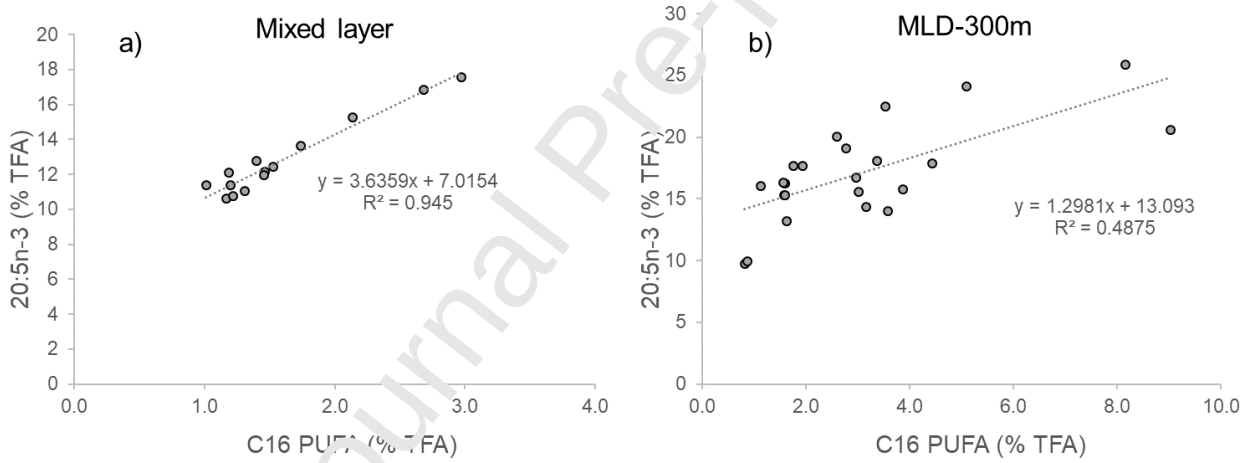

Figure 8: Correlation between diatoms C16 PUFA and 20:5n-3 proportions (% of total fatty acid-TFA) for the mixed layer (ML) (a) and for ML depth (MLD)-300m depth interval (b).

As diatoms C16 PUFA and 20:5n-3 were gathered in the PCA, we explored further this relationship in Figure 8. For the ML (Fig. 8a), C16 PUFA and 20:5n-3 appeared highly related regardless of stations (R^2=0.945, p<0.001). The slope of the regression indicated an average ratio of 20:5n-3 to C16 PUFA of 3.6±0.2, substantially higher than the ratio obtained for four diatom classes (Bacillariophyceae, Cosciondiscophycea, Fragilariophycea, and Mediophycea) gathered from literature (see Table S1), which ranged from 0.9 to 1.6. Considering the MLD-300m depth interval (Fig. 8b), the correlation between C16PUFA and 20:5n-3 was lower but still significant (R^2=0.487, p<0.001) and the average 20:5n-3 to C16 PUFA ratio decreased to 1.6±0.2.

n-3 C18 PUFA and 22:6n-3

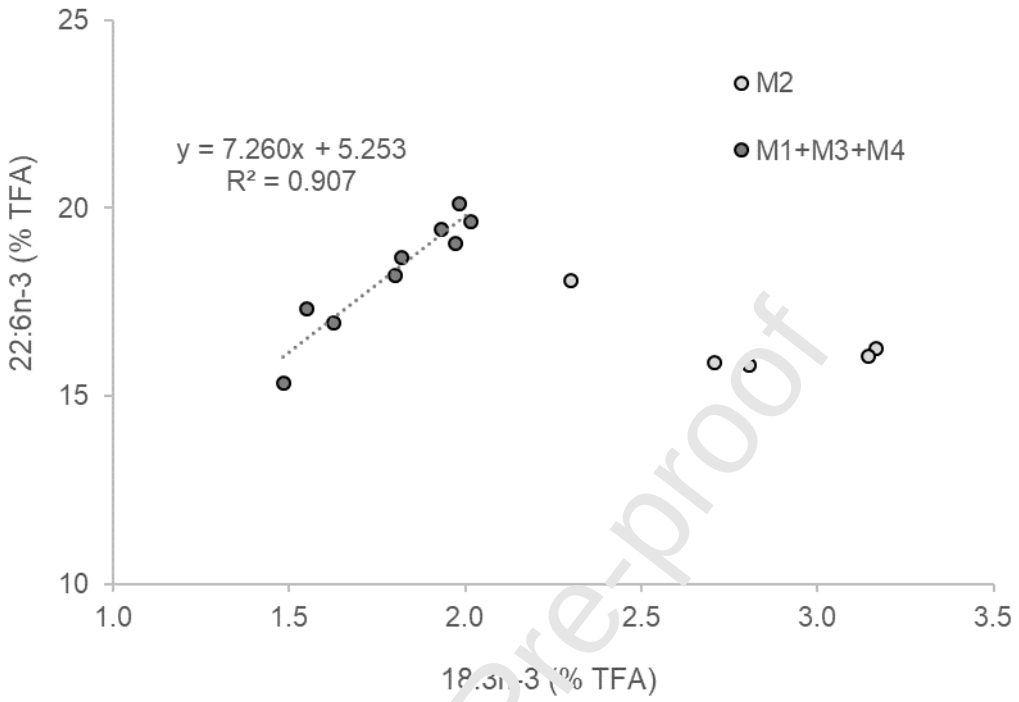

Figure 9: Linear regressions between 18:3n-3 and 22:6n-3 (% total fatty acid-TFA) in the mixed layer for off-plateau stations (M1, M3 and M4) and on-plateau station (M2).

From the PCA, 22:6n-3 was poorly correlated to axis 1 (R^2=12.5%, $p<0.05$) and not correlated to axes 2 and 3 when considering all stations and depths together. To further explore the relationship with non-diatom markers, we plotted in Figure 9 18:3n-3 against 22:6n-3 proportions in the ML. Although the numbers of data points reduced its statistical strength, separating the samples according to station locations (off-Plateau versus on-Plateau) allowed to obtain a significant (R^2=0.907, $p<0.001$) positive relationship between 18:3n-3 and 22:6n-3 for off-plateau stations (M1, M3, and M4). For the on-plateau station M2, the relationship was not significant (p=0.17) although 18:3n-3 and 22:6n-3 were negatively correlated.

22:6n-3 to n-3 C18 PUFA ratio increased linearly with depth between the surface and 300 m (R^2=0.726, p<0.0001; Figure 10). Significant relationships were observed between 22:6n-3/n-3 C18

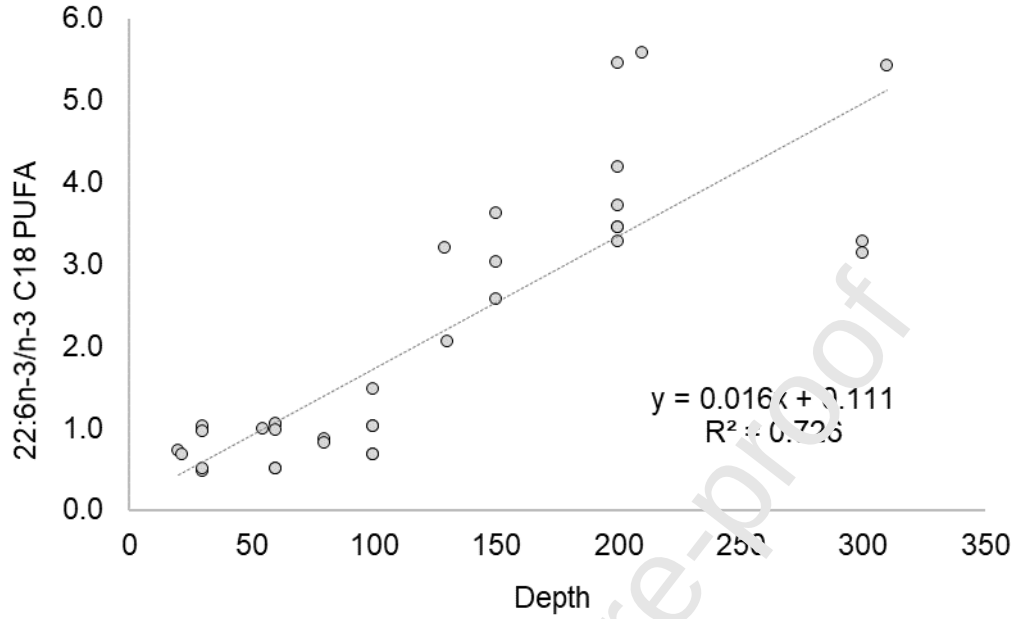

Figure 10: Linear regression between 22:6n-3 to n-3 C18 PUFA ratio according to depth (m).

PUFA ratio and 22:5n-3 and 20:1n-9 (R^2=0.874 with p<0.0001 and R^2=0.551 with p<0.001, respectively) are shown in Figure S2.

FA-based nutritional quality of SPOM

The nutritional quality index (NQI) deduced from FA is presented in Figure 11. NQI ranged from 354 to 477 (average 394±37) and did not vary significantly according to depth zones. It has to be noted that NQI was more variable with increasing depth. When considering together the

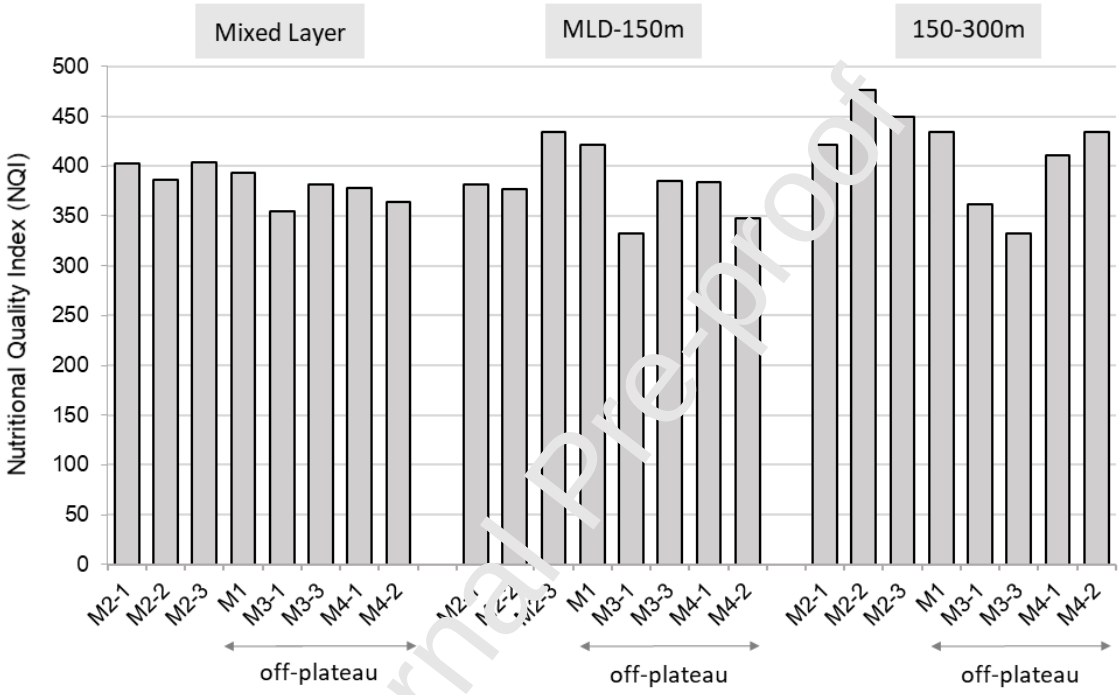

Figure 11: FA-based nutritional quality index of SPOM (1-50 μm) according to stations and depth intervals.

three depth zones, NQI was slightly higher on-plateau than off-plateau.

D. Discussion

This study investigated the upper water column distribution of 36 FA in SPOM (1-50 μm) collected in the Indian sector of the Southern Ocean in the region of Kerguelen Islands. Principal component analysis (PCA) revealed contrasted FA profiles attributable to depth for both PC1 and 2. The PC3 also revealed significant differences between HNLC stations M3 and M4 and the naturally-iron fertilized station M2. In the following, we discuss first how the post-bloom phytoplanktonic community and depth impact the FA composition of SPOM in terms of SC-

PUFA and MUFA. We then consider the potential sources of essential LC-PUFA, 20:5n-3 and 22:6n-3, in the ML and their fate in the upper mesopelagic. Finally, the FA-based nutritional quality of SPOM is discussed according to depth and stations location.

Post-bloom phytoplankton community and FA profiles

The MOBYDICK survey took place in late summer/early autumn coinciding with post-bloom conditions on and off the Kerguelen Plateau. Chl-a was low in the ML (<0.6 $\mu g.L^{-1}$), and POC and TFA concentrations were <45 $mg.L^{-1}$ and <4.5 $\mu g.L^{-1}$, respectively. The phytoplanktonic community, as described using 18S rDNA amplicon sequencing, pigments, flow cytometry, and microscopic enumeration (Irion et al., 2021, 2020; Lafond et al., 2020), revealed a mixed composition with three main groups, prymnesiophytes, diatoms and prasinophytes showing variable proportions on- and off the Plateau. Nano-phytoplankton (prymnesiophytes) were the most abundant group (37–53% and 59–70% of total Chl-a on- and off-plateau, respectively) followed by diatoms (27-40% and 18-33% of total Chl-a on- and off-plateau, respectively), and finally by pico-phytoplankton (prasinophytes) (Irion et al., 2021, 2020). This latter group was found in low proportions at all stations except on the plateau where it reached up to 16% of total Chl-a at the end of the survey (M2-3) (Irion et al., 2020). The mixed composition of the phytoplankton community was well reflected in the FA profile of SPOM, especially when considering chloroplastic C16 and n-3 C18 PUFA (Alonso et al., 1998; Guschina and Harwood, 2006), which derive mainly from autotrophic biomass. n-3 C18 PUFA (sum of 18:3n-3, 18:4n-3, and 18:5n-3) are characteristic of non-diatom phytoplankton including prymnesiophytes (24% of n-3 C18 PUFA) and prasinophytes (42% n-3 C18 PUFA), and were particularly abundant in the ML representing between 17 to 32% of TFA. n-3 C18 PUFA in the ML were significantly ($p<0.05$) higher on the Plateau (30±4% on average at station M2) and downstream (26% at M1) in comparison to HNLC off-plateau stations (19±4% on average at stations M3 and M4). On the Plateau, n-3 C18 PUFA increased from 22% (M2-1) to 32% (M2-2 and M2-3) during the survey probably illustrating the increasing proportion of Prasinophytes.

For diatoms, their abundance could be identified using C16 PUFA (sum of 16:2n-7, 16:2n-4, 16:3n-4 and 16:4n-1), which are highly specific to this phylum with an averaged proportion of

16±4% (see Table S1 for details). Diatom C16 PUFA were found at all stations in the ML. C16 PUFA were the lowest on the Plateau at station M2 (1.2±0.2% on average) and upstream at station M3 (1.3±0.2% on average) and were significantly ($p<0.05$) higher upstream at station M4 (2.3±0.6% on average) compared to the other stations. Variability of C16 PUFA according to stations in the ML could be compared to estimates of diatom abundance deduced from pigments (Irion et al., 2020), diatom biomass contribution to POC as well as BSi (Lafond et al., 2020). For off-plateau stations (M1, M3, and M4), C16 PUFA matched the trends in BSi concentrations (2.2 $\mu mol.L^{-1}$ at M4 > 1.0 $\mu mol.L^{-1}$ at M1 > 0.4 $\mu mol.L^{-1}$ at M3) as well as diatom contribution to POC (24±6% at M4 > 16±1% at M1 > 6±2% at M3). On the Plateau, differences arose and C16 PUFA proportions were the lowest while diatoms were found to be more abundant, 27-40% of total Chl-a (Irion et al., 2020) and 17 to 43% of POC (Lafond et al., 2020). This was especially the case at the last visit on the Plateau (station M2-3), where a bloom of *Corethron inerme* was observed (Lafond et al., 2020) which contributed to an increase of TFA and POC concentrations (2.1 to 2.9 $\mu g.L^{-1}$ and 27 to 40 $\mu g.L^{-1}$, respectively). In contrast, this effect was not reflected in C16 PUFA, whose proportions stayed relatively stable between station M2-2 (1.0%) and M2-3 (1.2%). This pattern could indicate that this late summer diatom bloom was probably poor in chloroplastic C16 PUFA.

Changes in FA profiles with depth

Below the ML, TFA and POC decreased rapidly and substantial changes were evidenced at all stations with a consistent decrease in n-3 C18 PUFA (from 24 ± 6% in the ML to 16 ± 6% in the MLD-150m down to 5 ± 1% in the 150-300 m depth zones) and an increase in C16 PUFA (from 1.6 ± 0.6% in the ML to 3.5 ± 1.1% in the MLD-150m and to 3.1 ± 1.4 % in the 150-300 m intervals). The observed pattern in phytoplankton-derived FA was in agreement with the vertical distribution of pigments showing a rapid decrease in prymnesiophytes pigments below the ML and an increasing contribution of diatom pigments, the latter representing up to 77-96% of total Chl-a at 250 m depth (Irion et al., 2021). In addition, we noted variable vertical trends of n-3 C18 PUFA and C16 PUFA as observed with pigments (Irion et al., 2021). On the Plateau and downstream (Station M2 and M1) n-3 C18 PUFA decreased rapidly below the MLD, while at

station M3 C18 PUFA remained relatively high in the MLD-150m depth interval (22% on average) and decreased only below 150 m (6% on average). For C16 PUFA and diatoms, the increase with depth was particularly rapid on the Plateau at the first two visits (1.5 to 5.5% at M2-1 and 1.0 to 4.3% at M2-2 between the ML and the MLD-150m depth zone) indicating an important accumulation of diatoms just below the MLD. Considering that biomass and associated FA increased below the ML as a result of vertical transfer from the surface, the observed trends in n-3 C18 PUFA and C16 PUFA proportions may be consistent with a more efficient export of diatoms in comparison to nano- and pico-phytoplankton below the ML. This feature is commonly observed in the SO (Salter et al., 2012, 2007) and was documented in details on the Plateau (Blain et al., 2021; Rembauville et al., 2015a, 2015b) and also in the surrounding HNLC areas (Rembauville et al., 2017).

Unexpectedly and along with n-3 C18 PUFA, the MUFA 17:1n-7 decreased linearly with depth. As its distribution was concomitant with the one of chloroplastic n-3 C18 PUFA, it suggested its production was mostly autotrophic and occurred in the ML. 17:1n-7 is not listed in the meta-analysis of Jónasdóttir (2019) and Cañavate (2019) and is only rarely cited in papers analyzing FA in phytoplankton species. The cyanobacteria *Synechococcus elongates*, *Microcystis aeruginosa* and *Anabaena variabilis* were reported to contain respectively 0.6%, 0.5% and 1.3 of 17:1n-7 (Bec et al., 2006; Martin-Creuzburg et al., 2008). Interestingly, the heterotrophic nanoflagellates *Paraphysomonas sp.*, concentrated this MUFA at 3.4% and 1.5%, when fed *S. elongates*, *M. aeruginosa* respectively (Bec et al., 2006). Indeed, these planktonic groups were observed during the MOBYDICK survey. Heterotrophic nanoflagellates, pico and nano-plankton varied between 3.3 and 4.7 10^6 cells.L^{-1}, 0.8 and 2.0 10^6 cells.L^{-1}, and 73 and 111 10^3 cells.L^{-1} respectively, in the ML (Christaki et al., 2020). However, while heterotrophic nanoflagellates were more abundant at M2 than at off-plateau stations (M3 and M4) (Christaki et al., 2020), no significant difference was observed according to stations for both concentration (in μg.L^{-1}) and relative proportion of 17:1n-7.

The long chain MUFA 20:1n-9, 22:1n-7 and 22:1n-9, which are mainly produced by zooplankton such as calanoid copepods and other crustaceans (Brett et al., 2009; Dalsgaard et al.,

2003; Kattner and Hagen, 1995; Mayzaud et al., 2007; Parrish, 2013; Wilson et al., 2010) can be used to detect potential interactions with zooplankton via the production of fecal pellets and their presence into SPOM (Mayzaud et al., 2007; Sheridan et al., 2002; Wilson et al., 2010). Fecal pellets are known to play an important role in the vertical transfer of OM in the Kerguelen region (Ebersbach and Trull, 2008; Laurenceau-Cornec et al., 2015), particularly on the Plateau during the post-bloom period (Rembauville et al., 2015a). In our samples, long chain MUFA 20:1n-9, 22:1n-7 and 22:1n-9 were detected at all stations, their proportions were low in the ML (sum of 20:1n-9, 22:1n-7, and 22:1n-9 ranging between 0.11 and 0.25%) and increased linearly with depth (R^2=0.683, p<0.0001) reaching the highest values in the 150-300m depth zone (range: 0.21-0.61%). Although particularly low, these proportions still appeared comparable to those measured in fecal pellets of copepods and euphausiids (range: 1.3-2.2%) sampled in the Subantarctic zone of the SO (Mayzaud et al., 2007). This could indicate that a fraction of the SPOM sampled during the post-bloom period was composed of fecal material excreted by zooplankton, which increased with depth. Moreover, and as outlined in the PCA, the PUFA 22:5n-3 was clearly associated with long chain MUFA. Indeed, a similar linear increase of 22:5n-3 with depth (R^2=0.79, p<0.001) was reported suggesting a common origin. This PUFA can be formed from the 20:5n-3 through elongation and could be a synthesis intermediate of 22:6n-3 in crustaceans including copepods (Kabeya et al., 2021; Monroig and Kabeya, 2018; Nielsen et al., 2019). This PUFA was found in three zooplankton species *Themisto libellula*, *Calanus marshallae/glacialis* (*Calanus spp.*), and *Thysanoessa raschii* collected in the Bering Sea and ranged between 0.5-0.6% of TFA (Wang et al., 2015). As part of MOBYDICK, 22:5n-3 accounted on average for 0.77% of total phospholipids extracted from 70 zooplankton samples (Puccinelli E. in prep) and its abundance in SPOM reached 1.3±0.1% on average in the 150-300m depth interval.

Origin and fate of 20:5n-3

Synthesis of the LC-PUFA 20:5n-3 is assumed to occur essentially via autotrophy and can be performed by several phytoplankton phyla such as Diatoms, ochrophytes, haptophytes, and rhodophytes (see Table S1 for details). In the ocean and in particular the SO, the main suppliers of 20:5n-3 are generally considered to be diatoms (Ericson et al., 2018; Hellessey et al., 2020). In

the case of MOBYDICK and for the Kerguelen area, this assumption seems to be true. 20:5n-3 was clearly associated with diatom C16 PUFA in the PCA and furthermore in the ML, proportions of 20:5n-3 appeared tightly related to C16 PUFA through a positive linear correlation (R^2=0.945, $p<0.05$) regardless of stations. Abundance of 20:5n-3 accounted for a significant contribution to TFA in the ML (13±2% on average), highest proportions were found at station M4 (15±2% on average), significantly ($p<0.001$) different in comparison to stations M2 and M3 (12±1% on average at both stations) and to a lesser extent to station M1 (14% on average). Measured proportions in 1-50 µm SPOM were comparable to literature data for diatoms ranging from 15 to 20% of 20:5n-3 (see details in Table S1). However, the literature range corresponds to diatoms monoculture and differs from the MOBYDICK situation. Because diatoms were a minor group in the ML (18–40% of total Chl-a) (Irion et al., 2020), proportions of 20:5n-3 in SPOM are expected to be lower compared to literature data if only provided by diatoms. Based on the highly significant linear relationship ($p<0.001$) between 20:5n-3 and diatoms C16 PUFA in the ML, we calculated a 20:5n-3/C16 PUFA ratio of 3.6±0.2, which appeared to be ~2 fold higher compared to literature data (average of 1.5 calculated from Table S1). This difference suggests that the diatom community of the Kerguelen region, both on and off-Plateau, had higher proportions of 20:5n-3 than cultured diatoms. Such a case was previously reported by Vaezi et al. (2013), who found that the cold-water *Fragilariopsis cylindrus* was able to produce up to 31.1% of 20:5n-3, approximately twice the average value usually found in the literature (Table S1). Additionally, we reported a significant negative regression between 20:5n-3 and temperature in the ML (R^2=44%, $p<0.01$). Indeed, 20:5n-3 proportion was the highest at station M4 where temperature was the lowest. Based on literature data, Hixson and Arts (2016) established a negative linear regression between temperature and 20:5n-3 in diatoms. Thus, it can be speculated that the high 20:5n-3 content in diatoms of the Kerguelen region partially reflected homeoviscous adaptation to low temperatures.

In the upper mesopelagic, relative proportions of 20:5n-3 increased, reaching 17±2% in the MLD-150m zone and 19±3% in the 150-300m zone, and were significantly ($p<0.001$) different compared to the ML. Linear relationship between C16 PUFA and 20:5n-3 was still significant below the MLD (R^2=0.487, $p<0.001$) with an average ratio 20:5n-3/C16 PUFA of 1.3. This ratio

was lower than in the ML and closer to the literature value (1.5, calculated from Table S1). This suggests that the vertical distribution of 20:5n-3 was still mostly determined by the fate of diatoms in the mesopelagic with no significant difference among stations. Accordingly, trends in 20:5n-3 proportions were likely a result of the increasing proportion of diatoms observed below the MLD. However, according to the low 20:5n-3/C16 PUFA ratio, the FA composition of diatoms has probably been modified with depth, and this could be related to several factors. For instance, diatoms assemblages exhibited consistent variations according to stations and depth (Lafond et al., 2020). This was particularly the case at the plateau station M2, where in the ML diatom biomass was dominated by the large centric *Corethron inerme* (59 to 83% of diatom biomass), while below the ML, *Eucampia antarctica* at the first visit (M2-1), and *Chaetoceros* resting spores and *Chaetoceros spp.* at the following visits (M2-2 and M2-3) were the dominant contributors (Lafond et al., 2020). At other stations, the community structure was more diverse and included *Actinocyclus spp.*, *Thalassiosira spp.* *Chaetoceros atlanticus* and *Chaetoceros* resting spores (Lafond et al., 2020). Considering that the amount of 20:5n-3 produced varies at a species level, diatom diversity were thus likely to influence the FA content available. Other factors could also involve the physiological state of diatom cells, which greatly evolved in the upper mesopelagic zone as a consequence of grazing, parasitic infection and mortality (Lafond et al., 2020; Sassenhagen et al., 2020). Indeed, abundance of detrital cells in the form of empty, broken or crushed frustules rapidly increased below the ML and this was particularly pronounced at off-plateau stations M1, M3, and M4 in comparison to on-plateau station M2, where up to 48% of cells were still intact between 175-200 m depth (Lafond et al., 2020). Finally, the relative proportions of 20:5n-3 as well as 20:5n-3/C16 PUFA ratio could have been modified as a result of the increasing proportion of fecal material observed in the mesopelagic zone. The FA composition of fecal pellets reflects the composition of the zooplankton organism (Hamm et al., 2001; Mayzaud et al., 2007) and can contain high and variable proportions of 20:5n-3 (up to 25-30%) as observed in krill (Hellessey et al., 2020), with substantial differences in comparison to the phytoplankton food source.

Origin and fate of 22:6n-3

The LC-PUFA 22:6n-3 is also produced at the basis of the marine food web by unicellular eukaryotic organisms (Dalsgaard et al., 2003; Parrish, 2013) and it is produced by several phytoplankton taxa (as detailed in Table S1). The taxa with the highest 22:6n-3 proportions, grown in autotrophic conditions, include Dinophyceae (17.5% in average), Coccolithophyceae (11.6% in average) and Prymnesiophyceae (10.7% in average) and exclude diatoms, which produce only small amounts of 22:6n-3 (<2.5%). In this study and considering first the ML, where autotrophic production was likely dominant, the 1-50 μm SPOM was found to be rich in 22:6n-3 at all stations representing 18±1% on average. The highest proportions were found off the Plateau at stations M1 and M3, with 19.1% and 19.5±0.5%, respectively, which were slightly higher to the upstream station M4 (17.0±1.0% in average) and the on-plateau station M2 (16.4±0.8% in average). According to the composition of the post-bloom phytoplankton community (Irion et al., 2021, 2020), it can be hypothesized that Prymnesiophycea, as the dominant group, were the most important suppliers of 22:6n-3 in the ML both on and off-Plateau. Autotrophic dinoflagellates (Dinophyceae), which are generally considered as important producers in the SO (Dalsgaard et al., 2003; Ericson et al., 2018; Falk-Petersen et al., 2000) were likely marginally involved as their contribution to the phytoplankton community was very modest (Irion et al., 2020). In addition to Prymnesiophyceae, contribution of pico-phytoplankton (Prasinophyceae) to 22:6n-3 proportions was also probable, especially on the Plateau where they were more abundant. Prasinophyceae are able to produce 22:6n-3 but in much lower proportions (7.0%) compared to Prymnesiophyceae. In order to test the assumption that Prasinophyceae and Prymnesiophyceae contributed to 22:6n-3 production, we considered the relationship between 22:6n-3 and 18:3n-3 in the ML. 22:6n-3 appeared strongly related to 18:3n-3 only at off plateau stations (M1, M3, and M4) through a positive correlation (R^2=0.907, $p<0.05$). The slope of the regression corresponding to the averaged 22:6n-3/18:3n-3 ratio found in off Plateau SPOM was 7.2 and was substantially higher than the ratio deduced from literature data for Prymnesiophycea (2.1) and Prasinophycea (0.6). The fact that the SPOM 22:6n-3/18:3n-3 ratio was closer to that of Prymnesiophyceae may indicate that 22:6n-3 was at least partially produced by Prymnesiophyceae rather than Prasinophyceae at these off-Plateau stations. The situation was markedly different on the Plateau at station M2, where 22:6n-3 and 18:3n-3 were

negatively related but not significantly, suggesting a more complex pattern. The observed trend in SPOM could be consistent with a multiple origin of 22:6n-3 with some from Prymnesiophyceae having a high 22:6n-3/18:3n-3 ratio and some from Prasinophyceae having a low 22:6n-3/18:3n-3 ratio. Different contributions of Prymnesiophycea and Prasinophyceae on and off Plateau seemed to be confirmed by the decrease of 22:6n-3/18:3n-3 ratio in SPOM observed at station M2 according to visits (7.9 at M2-1, 5.7 at M2-2, and 5.1 at M2-3) which fits with the increasing proportion of Prasinophyceae deduced from pigments and reaching up to 16% of total Chl-a at M2-3 (Irion et al., 2020).

Considering Prymnesiophycea, it is worth noting that this group was mostly composed by a single species, *Phaeocystis antarctica* (Irion et al., 2020), whose FA profile remains to be documented. As a comparison, data available for other species of *Phaeocystis* (*pouchetti* and *globosa*) exhibit contrasted FA profiles, with some studies reporting only trace or minor amounts of 22:6n-3 (maximum 6.2% TFA) (Claustre et al., 1990, Nichols et al., 1991; Skerratt et al., 1995), while others reported much higher proportions, up to 15% (Hamm et al., 2001; Sargent et al., 1985; Virtue et al., 1993). In our case, *Phaeocystis antarctica* was necessarily high in 22:6n-3 to match the high proportions observed in the ML (18±1% on average) and further work is needed to confirm this hypothesis.

In addition to autotrophic origin, trophic upgrading by heterotrophic protists such as dinoflagellates and ciliates, which composed the microzooplankton, may also have contributed to the observed 22:6n-3 content in the ML (Broglio et al., 2003; Lund et al., 2008). Heterotrophic dinoflagellates and ciliates were documented at both on and off-plateau stations and ranged between 0.29 and 2.3 10^3 cells L^{-1} (Christaki et al., 2021). Dinoflagellates, dominated by *Gymnodinium* sp., were more abundant than ciliates at all stations and grazed actively on phytoplankton with grazing rates exceeding phytoplankton growth rates (Christaki et al., 2021). Heterotrophic dinoflagellates can contain especially high proportions of 22:6n-3, >40% as reported by Lim et al. (2020) for *Gymnodinium smaydae*, and up to >50% for *Crypthecodinium cohnii* (Jiang and Chen, 2000). Interestingly for this latter species, 22:6n-3 proportions were dependent on cultivation temperature, increasing from 17% to 53% with decreasing temperature

from 30°C to 15°C (Jiang and Chen, 2000). Considering the low temperature environment of the Kerguelen region, this may have favored high 22:6n-3 proportions in heterotrophic protists. Another characteristic of heterotrophic dinoflagellates is their low content in chloroplastic n-3 C18 PUFA and as a consequence, their high 22:6n-3/n-3 C18 PUFA ratio (Lim et al., 2020; Lund et al., 2008). As an example, *Gymnodinium smaydae* had a 22:6n-3/18:3n-3 ratio >80, much higher than the ratio of its prey *Heterocapsa rotundata* of 5.4 (Lim et al., 2020). This may be one explanation for the higher 22:6n-3/18:3n-3 ratio found in the ML (7.2) in comparison to autotrophic producers (0.6-2.1) and could be consistent with a small contribution (<10%) of heterotrophic protists to 22:6n-3 content.

Below the ML in the upper mesopelagic, 22:6n-3 concentrations (in $\mu g.L^{-1}$) decreased substantially and similarly to TFA concentrations (R^2=0.975, $p<0.05$) it was maintained at high relative proportions with 17±2% in the MLD-150m depth interval comparable to the ML, and up to 20±2% in the 150-300m depth interval, significantly ($p<0.001$) higher in comparison to the upper layers. This vertical trend was in a marked contrast compared to n-3 C18 PUFA, which decreased substantially both in concentration and proportion below the ML. This contrasted pattern was initially outlined by the PCA, where 22:6n-3 was not correlated to any of the three axes and furthermore, not associated to n-3 C18 PUFA when considering the whole dataset. These different trends clearly indicate that the fate of 22:6n-3 in the mesopelagic could not be governed by the vertical transfer of non-diatom phytoplankton which was initially involved in its production in the ML, and most probably relied on another pathway. This pathway is further supported by the linear increase of 22:6n-3 to n-3 C18 PUFA ratio according to depth (R^2=0.726, $p<0.0001$) indicating a progressive enrichment of 22:6n-3 compared to n-3 C18 PUFA in SPOM between the surface and 300 m depth. Moreover, this increase correlates fairly well with the heterotrophic FA 22:5n-3 (R^2=0.874, $p<0.0001$) and also but to a lesser extent with the MUFA 20:1n-9 (R^2=0.551, $p<0.001$). Variations of 22:5n-3 and 20:1n-9 were attributed earlier in the discussion to an increasing abundance of fecal material at depth. Accordingly, it can be postulated that 22:6n-3 in SPOM may be at least partially associated with this fecal material in the upper mesopelagic and thus its fate may be controlled by interactions with the heterotrophic food web. It is worth noting that correlations were made regardless of stations, indicating that

this potential transfer pathway seemed to affect both iron-fertilized and HNLC regions. Such an association of 22:6n-3 with fecal material has already been documented in some regions of the world ocean, including the high latitude North Pacific where fecal OM and high proportions of 22:6n-3 (range 8-17% of TFA) were evidenced throughout the water column (Sheridan et al., 2002; Wilson et al., 2010) and also in the Arctic, where it was demonstrated that 22:6n-3 rich OM (~20% of TFA) derived from *Phaeocystis pouchetii,* was exported below the euphotic zone via krill fecal strings (Hamm et al., 2001).

In the present case, the processing of 22:6n-3 from phytoplankton to suspended fecal material is likely to be complex and could involve a number of heterotrophic intermediates. Among grazers, mesozooplankton such as copepods and other large size crustacean zooplankton require to be considered as C20-C22 MUFA are representative of fecal material excreted by these organisms (Brett et al., 2009; Dalsgaard et al., 2003; Kattner and Hagen, 1995; Mayzaud et al., 2007; Parrish, 2013; Wilson et al., 2010). Mesozooplankton were documented at all stations and exhibited significant variations according to sites and visits from 207 ind.m^{-3} at M2–1 to 1636 ind.m^{-3} at M4–1 (Christaki et al., 2021). Moreover, grazing experiments showed that copepods were not grazing directly on phytoplankton but were feeding primarily on microzooplankton controlling their abundance during the post-bloom period (Christaki et al., 2021). This feeding strategy on heterotrophic protists as well as the selective storage of 22:6n-3 as an essential LC-PUFA for mesozooplankton (Arendt et al., 2005) may have favoured its accumulation relative to n-3 C18 PUFA and as a result, impacted the composition of fecal material produced by these organisms. In addition to mesozooplankton, other grazers such as salps may also be involved in the channelling of 22:6n-3. Salps are important grazers of small phytoplankton (Moline et al., 2004) and flagellates (Pakhomov and Hunt, 2017; von Harbou et al., 2011), and produce easily fragmented tabular fecal pellets (Iversen et al., 2017). Salps population (*Salpa thompsoni*) were particularly abundant on the Plateau at station M2 and downstream at station M1 representing up to 40% of total micronekton biomass (Henschke et al., 2021).

Nutritional food value according to production regimes

The nutritional quality of OM as food for higher trophic levels is partly determined by the abundance of the essential omega-3 LC-PUFA 20:5n-3 and 22:6n-3 and the essential omega-6 20:4n-6. In the present study, LC-PUFA essentially composed of omega-3 LC-PUFA were found in high proportions, making up 27-44% of TFA, indicating a high nutritional value of SPOM both in the ML and upper mesopelagic. Following the approach developed by Cañavate et al. (2019), the NQI of SPOM was also high and ranged from 354 to 403 in the ML and from 333 to 477 in the MLD-300m depth interval. As a comparison, much lower NQI were obtained in the estuary of Guadalquivir River, with values always <200 (Cañavate et al., 2021), in the northern part of the Indian sector of the ACC, with NQI of 193 and 242 in surface SPOM of the subtropical and Subantarctic zone, respectively (Mayzaud et al. 2007), in the Northern Pacific, NQI was <300 in >51 μm SPOM of the Subarctic area (Wilson et al., 2010) as well as in the coastal Antarctic zone, NQI was <260 for a diatom sea-ice community of McMurdo Sound (Nichols et al., 1993). This comparison confirms that quality of SPOM in the Kerguelen area was especially high in the post-bloom period. High NQI values were observed over the whole area and seemed unrelated to the contrasted productivity regimes that took place earlier in the season during the bloom. In the ML, the high nutritional value of SPOM was mainly attributable to the mixed phytoplanktonic community relying both on diatoms producing 20:5n-3 and small phytoplankton producing 22:6n-3. This mixed production of both LC-PUFA substantially promoted the nutritional quality of SPOM and offered a valuable source of food for secondary consumers that could be of importance for the ecosystem functioning.

In the upper mesopelagic, LC-PUFA in SPOM were maintained at similar, and even higher, proportions in comparison to the ML (34±2% and 40±3% on average in the MLD-150m and 150-300m depth intervals, respectively). Similarly, NQI remained high until 300 m depth (333-477) even though TFA concentrations in seawater (in $\mu g.L^{-1}$) decreased substantially with depth. This preservation of food quality in the upper mesopelagic was rather unexpected because LC-PUFA are generally considered as a labile fraction of OM that could be easily degraded/consumed by heterotrophic organisms during their transfer from the surface (Budge et al., 2006; Conte et al., 2003, 1995; Wakeham, 1995). This is illustrated by the low NQI values that can be deduced from sediment trap data, with values between 90 to 180 in trap samples collected between 50-100 m

depth in the North Atlantic (Budge and Parrish, 1998) and NQI <30 in samples collected at 300 m depth in Breid Bay, Antarctica (Hayakawa et al., 1996). For the Kerguelen region, sediment trap data obtained on the Plateau at station M2 (Rembauville et al., 2018) do not allow for NQI estimates, however considering LC-PUFA concentrations per unit mass of OC, ranging from 0.03 to 3.4 μg.mgOC^{-1} in the trap samples and from 14 to 44 μg.mgOC^{-1} in our SPOM samples, it appears that sinking material from traps was of much lower quality than suspended particles collected on and off the Plateau. In the present case, the high quality of SPOM in the upper mesopelagic could represent a valuable nutritional option for heterotrophic organisms residing in the part of the water column and feeding on suspended particles such as zooplankton, coprophages, detritivores, and bacteria.

E. CONCLUSION

In this study, FA distribution including essential LC-PUFA 20:5n-3 and 22:6n-3 was documented in the upper water column of the Kerguelen Islands Region several weeks after the bloom period in late summer/early autumn. Our results illustrate the important role of the mixed phytoplankton community, composed of nano- and pico-size phytoplankton and diatoms, in providing high proportions of both LC-PUFA to surface waters. Diatoms were identified as the likely suppliers of 20:5n-3 and small phytoplankton (prymnesiophytes and prasinophytes) supplying 22:6n-3. Elevated proportions are unrelated to past productivity regimes and were observed both inside the iron-fertilized area on the Kerguelen Plateau (station M2) and downstream (station M1), as well as outside in HNLC waters located upstream of the Plateau (stations M3 and M4). As a consequence, and despite reduced productivity and biomass abundance during the post-bloom period, phytoplankton-derived OM reveal an especially high nutritional value that could be relevant for secondary consumers such as micro- and mesozooplankton.

In the upper mesopelagic, both LC-PUFA were maintained at high relative proportions in SPOM suggesting an efficient and probably fast vertical transfer from the surface. This vertical transfer seems to proceed via distinct pathways according to LC-PUFA. For 20:5n-3, its fate in the mesopelagic seems to mainly follow the one of diatoms and could be associated with the

export of large intact cells, diatoms aggregates as well as resting spores. For 22:6n-3, its fate with depth appears not to be simply related to small phytoplankton but is most likely due to a complex channeling through the heterotrophic food web resulting in its association with fecal material at depth. Processing of 22:6n-3 could involve different intermediates such as heterotrophic protists with dinoflagellates and ciliates (microzooplankton), which probably grazed on small phytoplankton as well as larger zooplankton organisms such as copepods and salps, which presumably fed on microzooplankton and produced fecal pellets rich in 22:6n-3. The complex pathway of 22:6n-3 cannot be easily resolved using only SPOM data and additional evidences are needed to better understand this pattern. Despite these contrasted pathways, FA-based nutritional quality of SPOM remained especially high in the upper mesopelagic and could represent an interesting food source for suspension feeders residing there. Finally, these results provide a detailed framework of FA abundances that can be used in trophic and diet studies dedicated to the Subantarctic islands.

F. Acknowledgments

We thank B. Quéguiner, the PI of the MOBYDICK project, for providing us the opportunity to participate to this cruise, the chief scientist I. Obernosterer and the captain and crew of the R/V Marion Dufresne for their enthusiasm and support aboard during the MOBYDICK–THEMISTO cruise (https://doi.org/10.17600/18000403). This work was supported by the French oceanographic fleet ("Flotte oceanographique française"), the French ANR ("Agence Nationale de la Recherche", AAPG 2017 program, MOBYDICK Project number: ANR-17-CE01-0013), the French Research program of INSU-CNRS LEFE/CYBER ("Les enveloppes fluides et l'environnement" – "Cycles biogéochimiques, environnement et ressources"). Marine Remize PhD fellowship and studies was supported by the University of Brest (UBO, France), the Center of Marine Sciences (CMS) of the University of North Carolina Wilmington (UNCW, USA), the "Laboratoire d'Excellence" LabexMer (ANR-10-LABX-19), and the Walter-Zellidja grant of the Académie Française. E. Puccinelli was supported by ISblue project, Interdisciplinary graduate school for the blue planet (ANR-17-EURE-0015) and co-funded by a grant from the French government under the program "Investissements d'Avenir". We would like to thank our

colleagues of the Technical Division of the INSU, Emmanuel de Saint-Leger, Lionel Scouarnec, Lionel Fischen, and Olivier Desprez De Gesincourt for their logistical and technical help with the in-situ pumps, the colleagues of the UBO Open Factory for their help in designing and preparing the NITEX membranes, and also to Stephane Blain and Bernard Quéguiner for their helpful comments and suggestions on the manuscript.

Declaration of interests

☒ The authors declare that they have no known competing financial interests or personal relationships that could have appeared to influence the work reported in this paper.

☐ The authors declare the following financial interests/personal relationships which may be considered as potential competing interests:

References

Alonso, D.L., Belarbi, E.-H., Rodríguez-Ruiz, J., Segura, C.I., Giménez, A., 1998. Acyl lipids of three microalgae. Phytochemistry 47, 1473–1481. https://doi.org/10.1016/S0031-9422(97)01080-7

Arendt, K.E., Jónasdóttir, S.H., Hansen, P.J., Gärtner, S., 2005. Effects of dietary fatty acids on the reproductive success of the calanoid copepod Temora longicornis. Marine Biology 146, 513–530. https://doi.org/10.1007/s00227-004-1457-9

Armand, L.K., Cornet-Barthaux, V., Mosseri, J., Quéguiner, B., 2008. Late summer diatom biomass and community structure on and around the naturally iron-fertilised Kerguelen Plateau in the Southern Ocean. Deep Sea Research Part II: Topical Studies in Oceanography 55, 653–676. https://doi.org/10.1016/j.dsr2.2007.12.031

Atkinson, A., Shreeve, R.S., Hirst, A.G., Rothery, P., Tarling, G.A., Pond, D.W., Korb, R.E., Murphy, E.J., Watkins, J.L., 2006. Natural growth rates in Antarctic krill (Euphausia superba): II. Predictive models based on food, temperature, body length, sex, and maturity stage. Limnology and Oceanography 51, 973–987. https://doi.org/10.4319/lo.2006.51.2.0973

Bec, A., Martin-Creuzburg, D., von Elert, E., 2006. Trophic upgrading of autotrophic picoplankton by the heterotrophic nanoflagellate Paraphysomonas sp. Limnology and Oceanography 51, 1699–1707. https://doi.org/10.4319/lo.2006.51.4.1699

Blain, S., Queguiner, B., Armand, L., Belviso, S., Bombled, B., Bopp, L., Bowie, A., Brunet, C., Brussaard, C., Carlotti, F., Christaki, U., Corbiere, A., Durand, I., Ebersbach, F., Fuda, J.-L., Garcia, N., Gerringa, L., Griffiths, B., Guigue, C., Guillerm, C., Jacquet, S., Jeandel, C., Laan, P., Lefevre, D., Lo Monaco, C., Malits, A., Mosseri, J., Obernosterer, I., Park, Y.-H., Picheral, M., Pondaven, P., Remenyi, T., Sandroni, V., Sarthou, G., Savoye, N., Scouarnec, L., Souhaut, M., Thuiller, D., Timmermans, K., Trull, T., Uitz, J., van Beek, P., Veldhuis, M., Vincent, D., Viollier, E., Vong, L., Wagener, T., 2007. Effect of natural iron fertilization on carbon sequestration in the Southern Ocean. Nature 446, 1070–1074. https://doi.org/10.1038/nature05700

Blain, S., Rembauville, M., Crispi, O., Obernosterer, I., 2021. Synchronized autonomous sampling reveals coupled pulses of biomass and export of morphologically different diatoms in the Southern Ocean. Limnology and Oceanography 66, 753–764. https://doi.org/10.1002/lno.11638

Blain, S., Sarthou, G., Laan, P., 2008. Distribution of dissolved iron during the natural iron-fertilization experiment KEOPS (Kerguelen Plateau, Southern Ocean). Deep Sea Research Part II: Topical Studies in Oceanography 55, 594–605. https://doi.org/10.1016/j.dsr2.2007.12.028

Brett, M.T., Müller-Navarra, D., 1997. The role of highly unsaturated fatty acids in aquatic food web processes. Freshwater Biology 38, 483–499. https://doi.org/10.1046/j.1365-2427.1997.00220.x

Brett, M.T., Müller-Navarra, D.C., Persson, J., 2009. Crustacean zooplankton fatty acid composition, in: Kainz, M., Brett, M., Arts, M. (Eds.), Lipids in Aquatic Ecosystems. Springer, New York, NY.

Broglio, E., Jónasdóttir, S.H., Calbet, A., Jakobsen, H.H., Saiz, E., 2003. Effect of heterotrophic versus autotrophic food on feeding and reproduction of the calanoid copepod Acartia tonsa: relationship with prey fatty acid composition. Aquat Microb Ecol 31, 267–278.

Brooks, P.D., Geilmann, H., Werner, R.A., Brand, W., 2003. Improved precision of coupled 13C and 15N measurements from single samples using an elemental analyser. Rapid Communications in Mass Spectrometry 12, 1924–1926. https://doi.org/10.1002/rcm.1134

Budge, S.M., Iverson, S.J., Koopman, H.N., 2006. Studying trophic ecology in marine ecosystems using fatty acids: a primer on analysis and interpretation. Marine Mammal Science 22, 759–801.

Budge, S.M., Parrish, C.C., 1998. Lipid biogeochemistry of plankton, settling matter and sediments in Trinity Bay, Newfoundland. II. Fatty acids. Organic Geochemistry 29, 1547–1559. https://doi.org/10.1016/S0146-6380(98)00177-6

Cañavate, J.P., 2019. Advancing assessment of marine phytoplankton community structure and nutritional value from fatty acid profiles of cultured microalgae. Reviews in Aquaculture 11, 527–549. https://doi.org/10.1111/raq.12244

Cañavate, J.-P., van Bergeijk, S., González-Ortegón, E., Vilas, C., 2021. Contrasting fatty acids with other indicators to assess nutritional status of suspended particulate organic matter in a turbid estuary. Estuarine, Coastal and Shelf Science 254, 107329. https://doi.org/10.1016/j.ecss.2021.107329

Cavagna, A.J., Fripiat, F., Elskens, M., Mangion, P., Chirurgien, L., Closset, I., Lasbleiz, M., Florez-Leiva, L., Cardinal, D., Leblanc, K., Fernandez, C., Lefèvre, D., Oriol, L., Blain, S., Quéguiner, B., Dehairs, F., 2015. Production regime and associated N cycling in the vicinity of Kerguelen Island, Southern Ocean. Biogeosciences 12, 6515–6528. https://doi.org/10.5194/bg-12-6515-2015

Christaki, U., Guenebaut, A., Liu, Y., Blain, S., Catala, P., Colombet, J., Debeljak, P., Jardillier, L., Irion, S., Planchon, F., Sassenhagen, I., Sime-Ngando, T., Obernosterer, I., 2020. Seasonal microbial food web dynamics in contrasting Southern Ocean productivity regimes. Limnology and Oceanography n/a. https://doi.org/10.1002/lno.11591

Christaki, U., Skouroliakou, I.-D., Delegrange, A., Irion, S., Courcot, L., Jardillier, L., Sassenhagen, I., 2021. Microzooplankton diversity and potential role in carbon cycling of contrasting Southern Ocean productivity regimes. Journal of Marine Systems 219, 103531. https://doi.org/10.1016/j.jmarsys.2021.103531

Claustre, H., Poulet, S.A., Williams, R., Marty, J.C., Coombs, S., Mlih, F.B., Hapette, A.M., Jezequel-Martin, V., 1990. A biochemical investigation of a Phaeocystis sp. bloom in the Irish Sea. Journal of the Marine Biological Association of the United Kingdom 70, 197–207. https://doi.org/10.1017/S0025315400034317

Constable, A.J., Melbourne-Thomas, J., Corney, S.P., Arrigo, K.R., Barbraud, C., Barnes, D.K.A., Bindoff, N.L., Boyd, P.W., Brandt, A., Costa, D.P., Davidson, A.T., Ducklow, H.W., Emmerson, L., Fukuchi, M., Gutt, J., Hindell, M.A., Hofmann, E.E., Hosie, G.W., Iida, T., Jacob, S., Johnston, N.M., Kawaguchi, S., Kokubun, N., Koubbi, P., Lea, M.-A., Makhado, A., Massom, R.A., Meiners, K., Meredith, M.P., Murphy, E.J., Nicol, S., Reid, K., Richerson, K., Riddle, M.J., Rintoul, S.R., Smith Jr, W.O., Southwell, C., Stark, J.S., Sumner, M., Swadling, K.M., Takahashi, K.T., Trathan, P.N., Welsford, D.C., Weimerskirch, H., Westwood, K.J., Wienecke, B.C., Wolf-Gladrow, D., Wright, S.W., Xavier, J.C., Ziegler, P., 2014. Climate change and Southern Ocean ecosystems I: how changes in physical habitats directly affect marine biota. Global Change Biology 20, 3004–3025. https://doi.org/10.1111/gcb.12623

Conte, M.H., Dickey, T.D., Weber, J.C., Johnson, R.J., Knap, A.H., 2003. Transient physical forcing of pulsed export of bioreactive material to the deep Sargasso Sea. Deep Sea Research Part I: Oceanographic Research Papers 50, 1157–1187. https://doi.org/10.1016/S0967-0637(03)00141-9

Conte, M.H., Eglinton, G., Madreira, L.A.S., Rabouille, C., Labeyrie, L., Mudge, S., Eglinton, G., Elderfield, H., Whitfield, M., Williams, P.J.Le.B., 1995. Origin and fate of organic biomarker compounds in the water column and sediments of the eastern North Atlantic. Philosophical Transactions of the Royal Society of London. Series B: Biological Sciences 348, 169–178. https://doi.org/10.1098/rstb.1995.0059

Dalsgaard, J., St. John, M., Kattner, G., Müller-Navarra, D., Hagen, W., 2003. Fatty acid trophic markers in the pelagic marine environment, in: Advances in Marine Biology. Academic Press, pp. 225–340. https://doi.org/10.1016/S0065-2881(03)46005-7

de Baar, H.J.W., de Jong, J.T.M., Bakker, D.C.E., Loscher, B.M., Veth, C., Bathmann, U., Smetacek, V., 1995. Importance of iron for plankton blooms and carbon dioxide drawdown in the Southern Ocean. Nature 373, 412–415. https://doi.org/10.1038/373412a0

Deppeler, S.L., Davidson, A.T., 2017. Southern Ocean Phytoplankton in a Changing Climate. Frontiers in Marine Science 4. https://doi.org/10.3389/fmars.2017.00040

Dunstan, G.A., Volkman, J.K., Barrett, S.M., Leroi, J.-M., Jeffrey, S.W., 1993. Essential polyunsaturated fatty acids from 14 species of diatom (Bacillariophyceae). Phytochemistry 35, 155–161. https://doi.org/10.1016/S0031-9422(00)90525-9

Ebersbach, F., Trull, T.W., 2008. Sinking particle properties from polyacrylamide gels during the KErguelen Ocean and Plateau compared Study (KEOPS): Zooplankton control of carbon export in an area of persistent natural iron inputs in the Southern Ocean. Limnol. Oceanogr. 53, 212–224. https://doi.org/10.4319/lo.2008.53.1.0212

El-Sayed, S.Z., 1988. Productivity of the southern ocean: a closer look. Comparative Biochemistry and Physiology Part B: Comparative Biochemistry 90, 489–498. https://doi.org/10.1016/0305-0491(88)90327-8

Ericson, J.A., Hellessey, N., Nichols, P.D., Kawaguchi, S., Nicol, S., Hoem, N., Virtue, P., 2018. Seasonal and interannual variations in the fatty acid composition of adult Euphausia superba Dana, 1850 (Euphausiacea) samples derived from the Scotia Sea krill fishery. Journal of Crustacean Biology 38, 662–672. https://doi.org/10.1093/jcbiol/ruy032

Evans, C., Brussaard, C.P.D., 2012. Viral lysis and microzooplankton grazing of phytoplankton throughout the Southern Ocean. Limnology and Oceanography 57, 1826–1837. https://doi.org/10.4319/lo.2012.57.6.1826

Fahl, K., Kattner, G., 1993. Lipid content and fatty acid composition of algal communities in sea-ice and water from the Weddell Sea (Antarctica). Polar Biology 13, 405–409. https://doi.org/10.1007/BF01681982

Falk-Petersen, S., Hagen, W., Kattner, G., Clarke, A., Sargent, J., 2000. Lipids, trophic relationships, and biodiversity in Arctic and Antarctic krill. Canadian Journal of Fisheries and Aquatic Sciences 57, 178–191. https://doi.org/10.1139/f00-194

Fiala, M., Kopczynska, E.E., Jeandel, C., Oriol, L., Vetion, G., 1998. Seasonal and interannual variability of size-fractionated phytoplankton biomass and community structure at station Kerfix, off the Kerguelen Islands, Antarctica. Journal of Plankton Research 20, 1341–1356. https://doi.org/10.1093/plankt/20.7.1341

Gillan, F.T., McFadden, G.I., Wetherbee, R., Johns, R.B., 1981. Sterols and fatty acids of an Antarctic sea ice diatoms, Stauroneis amphioxys. Phytochemistry 20, 1935–1937.

Guo, F., Bunn, S.E., Brett, M.T., Kainz, M., 2017. Polyunsaturated fatty acids in stream food webs - high dissimilarity among producers and consumers. Freshwater Biology 62, 1325–1334. https://doi.org/10.1111/fwb.12956

Guschina, I.A., Harwood, J.L., 2006. Lipids and lipid metabolism in eukaryotic algae. Progress in Lipid Research 45, 160–186. https://doi.org/10.1016/j.plipres.2006.01.001

Hamm, C., Reigstad, M., Riser, C.W., Mühlebach, Anneke, Wassmann, P., 2001. On the trophic fate of Phaeocystis pouchetii. VII. Sterols and fatty acids reveal sedimentation of P. pouchetii-derived organic matter via krill fecal strings. Mar Ecol Prog Ser 209, 55–69.

Hayakawa, K., Handa, N. Ikuta, N., Fukuchi, M., 1996. Downward fluxes of fatty acids and hydrocarbons during a phytoplankton bloom in the austral summer in Breid Bay, Antarctica. Organic Geochemistry 24, 511–521. https://doi.org/10.1016/0146-6380(96)00047-2

Hellessey, N., Johnson, R., Ericson, J.A., Nichols, P.D., Kawaguchi, S., Nicol, S., Hoem, N., Virtue, P., 2020. Antarctic Krill Lipid and Fatty acid Content Variability is Associated to Satellite Derived Chlorophyll a and Sea Surface Temperatures. Scientific Reports 10, 6060. https://doi.org/10.1038/s41598-020-62800-7

Hernando, M., Schloss, I.R., Almandoz, G.O., Malanga, G., Varela, D.E., De Troch, M., 2018. Combined effects of temperature and salinity on fatty acid content and lipid damage in

Antarctic phytoplankton. Journal of Experimental Marine Biology and Ecology 503, 120–128. https://doi.org/10.1016/j.jembe.2018.03.004

Hixson, S.M., Arts, M.T., 2016. Climate warming is predicted to reduce omega-3, long-chain, polyunsaturated fatty acid production in phytoplankton. Global Change Biology 22, 2744–2755. https://doi.org/10.1111/gcb.13295

Irion, S., Christaki, U., Berthelot, H., L'Helguen, S., Jardillier, L., 2021. Small phytoplankton contribute greatly to CO2-fixation after the diatom bloom in the Southern Ocean. The ISME Journal. https://doi.org/10.1038/s41396-021-00915-z

Irion, S., Jardillier, L., Sassenhagen, I., Christaki, U., 2020. Marked spatiotemporal variations in small phytoplankton structure in contrasted waters of the Southern Ocean (Kerguelen area). Limnology and Oceanography. https://doi.org/10.1002/lno.11555

Iversen, M.H., Pakhomov, E.A., Hunt, B.P.V., van der Jagt, H., Wolf-Gladrow, D., Klaas, C., 2017. Sinkers or floaters? Contribution from salp pellets to the export flux during a large bloom event in the Southern Ocean. Deep Sea Research Part II: Topical Studies in Oceanography 138, 116–125. https://doi.org/10.1016/j.dsr2.2016.12.004

Jiang, Y., Chen, F., 2000. Effects of medium glucose concentration and pH on docosahexaenoic acid content of heterotrophic Crypthecodinium cohnii. Process Biochemistry 35, 1205–1209. https://doi.org/10.1016/S0032-9592(00)00163-1

Jónasdóttir, S.H., 2019. Fatty Acid Profiles and Production in Marine Phytoplankton. Marine Drugs 17, 151.

Kabeya, N., Ogino, M., Ushio, H., Haga, Y., Satoh, S., Navarro, J.C., Monroig, Ó., 2021. A complete enzymatic capacity for biosynthesis of docosahexaenoic acid (DHA, 22 : 6n–3) exists in the marine Harpacticoida copepod Tigriopus californicus. Open Biology 11, 200402. https://doi.org/10.1098/rsob.200402

Kattner, G., Hagen, W., 1995. Polar herbivorous copepods – different pathways in lipid biosynthesis. ICES Journal of Marine Science 52, 329–335. https://doi.org/10.1016/1054-3139(95)80048-4

Klein-Breteler, W.C.M., Schogt, N., Baas, M., Schouten, S., Kraay, G.W., 1999. Trophic upgrading of food quality by protozoans enhancing copepod growth: role of essential lipids. Marine Biology 135, 191–198. https://doi.org/10.1007/s002270050616

Kopczyńska, E.E., Fiala, M., Jeandel, C., 1998. Annual and interannual variability in phytoplankton at a permanent station off Kerguelen Islands, Southern Ocean. Polar Biology 20, 342–351. https://doi.org/10.1007/s003000050312

Korb, R.E., Whitehouse, M., 2004. Contrasting primary production regimes around South Georgia, Southern Ocean: large blooms versus high nutrient, low chlorophyll waters. Deep Sea Research Part I: Oceanographic Research Papers 51, 721–738. https://doi.org/10.1016/j.dsr.2004.02.006

Lafond, A., Leblanc, K., Legras, J., Cornet, V., Quéguiner, B., 2020. The structure of diatom communities constrains biogeochemical properties in surface waters of the Southern Ocean (Kerguelen Plateau). Journal of Marine Systems 212, 103458. https://doi.org/10.1016/j.jmarsys.2020.103458

Lasbleiz, M., Leblanc, K., Armand, L.K., Christaki, U., Georges, C., Obernosterer, I., Quéguiner, B., 2016. Composition of diatom communities and their contribution to plankton biomass in the naturally iron-fertilized region of Kerguelen in the Southern Ocean. FEMS Microbiology Ecology 92, fiw171.

Laurenceau-Cornec, E.C., Trull, T.W., Davies, D.M., Bray, S.G., Doran, J., Planchon, F., Carlotti, F., Jouandet, M.P., Cavagna, A.J., Waite, A.M., Blain, S., 2015. The relative importance of phytoplankton aggregates and zooplankton fecal pellets to carbon export: insights from free-drifting sediment trap deployments in naturally iron-fertilised waters near the Kerguelen Plateau. Biogeosciences 12, 1007–1027. https://doi.org/10.5194/bg-12-1007-2015

Lim, A.S., Jeong, H.J., You, J.H., Park, S.A., 2020. Semi-continuous cultivation of the mixotrophic dinoflagellate Gymnodinium smaydae, a new promising microalga for omega-3 production. Algae 35, 277–292. https://doi.org/10.4490/algae.2020.35.9.2

Liu, Y., Blain, S., Crispi, O., Rembauville, M., Obernosterer, I., 2020. Seasonal dynamics of prokaryotes and their associations with diatoms in the Southern Ocean as revealed by an autonomous sampler. Environmental Microbiology 22, 3968–3984. https://doi.org/10.1111/1462-2920.15184

Lund, E.D., Chu, F.-L.E., Harvey, E., Adlof, R., 2008. Mechanism(s) of long chain n-3 essential fatty acid production in two species of heterotrophic protists: Oxyrrhis marina and Gyrodinium dominans. Marine Biology 155, 23–36. https://doi.org/10.1007/s00227-008-1003-2

Martin, J.H., 1990. Glacial-interglacial CO2 change: The Iron Hypothesis. Paleoceanography 5, 1–13. https://doi.org/10.1029/PA005i001p00001

Martin-Creuzburg, D., von Elert, E., Hoffmann, K.H., 2008. Nutritional constraints at the cyanobacteria—Daphnia magna interface: The role of sterols. Limnology and Oceanography 53, 456–468. https://doi.org/10.4319/lo.2008.53.2.0456

Mathieu-Resuge, M., Schaal, G., Kraffe, E., Corvaisier, R., Lebeau, O., Lluch-Costa, S.E., Salgado García, R.L., Kainz, M.J., Le Grand, F., 2019. Different particle sources in a bivalve species of a coastal lagoon: evidence from stable isotopes, fatty acids, and compound-specific stable isotopes. Marine Biology 166, 89–101.

Mayzaud, P., Laureillard, J., Merien, D., Brinis, A., Godard, C., Razouls, S., Labat, J. –P, 2007. Zooplankton nutrition, storage and fecal lipid composition in different water masses associated with the Agulhas and Subtropical Fronts. Marine Chemistry 107, 202–213. https://doi.org/10.1016/j.marchem.2007.07.001

Mayzaud, P., Tirelli, V., Errhif, A., Labat, J.P., Razouls, S., Perissinotto, R., 2002. Carbon intake by zooplankton. Importance and role of zooplankton grazing in the Indian sector of the Southern Ocean. Deep Sea Research Part II: Topical Studies in Oceanography 49, 3169–3187. https://doi.org/10.1016/S0967-0645(02)00077-2

Mitani, E., Nakayama, F., Matsuwaki, I., Ichi, I., Kawabata, A., Kawachi, M., Kato, M., 2017. Fatty acid composition profiles of 235 strains of three microalgal divisions within the NIES Microbial Culture Collection. Microb. Resour. Syst 33, 1929.

Moline, M.A., Claustre, H., Frazer, T.K., Schofield, O., Vernet, M., 2004. Alteration of the food web along the Antarctic Peninsula in response to a regional warming trend. Global Change Biology 10, 1973–1980. https://doi.org/10.1111/j.1365-2486.2004.00825.x

Mongin, M., Molina, E., Trull, T.W., 2008. Seasonality and scale of the Kerguelen plateau phytoplankton bloom: A remote sensing and modeling analysis of the influence of natural iron fertilization in the Southern Ocean. Deep Sea Research Part II: Topical Studies in Oceanography 55, 880–892. https://doi.org/10.1016/j.dsr2.2007.12.039

Monroig, Ó., Kabeya, N., 2018. Desaturases and elongases involved in polyunsaturated fatty acid biosynthesis in aquatic invertebrates: a comprehensive review. Fisheries Science 84, 911–928. https://doi.org/10.1007/s12562-018-1254-x

Müller-Navarra, D.C., Brett, M.T., Liston, A.M., Goldman, C.R., 2000. A highly unsaturated fatty acid predicts carbon transfer between primary producers and consumers. Nature 403, 74–77. https://doi.org/10.1038/47469

Nichols, D.S., Nichols, P.D., Sullivan, C.W., 1993. Fatty acid, sterol and hydrocarbon composition of Antarctic sea ice diatom communities during the spring bloom in McMurdo Sound. Antartic Science 5, 271–278.

Nichols, P.D., Skerratt, J.H., Davidson, A., Burton, H., McMeekin, T.A., 1991. Lipids of cultured Phaeocystis pouchetii: Signatures for food-web, biogeochemical and environmental studies in Antarctica and the Southern ocean. Phytochemistry 30, 3209–3214. https://doi.org/10.1016/0031-9422(91)83177-M

Nielsen, B.L.H., Gøtterup, L., Jørgensen, T.S., Hansen, B.W., Hansen, L.H., Mortensen, J., Jepsen, P.M., 2019. n-3 PUFA biosynthesis by the copepod Apocyclops royi documented using fatty acid profile analysis and gene expression analysis. Biology Open 8. https://doi.org/10.1242/bio.038331

Okuyama, H., Morita, N., Kogame, K., 1992. Occurrence of octadecapentaenoic acid in lipids of a cold stenothermic alga, prymnesiophyte strain B. Journal of Phycology 28, 465–472.

Orsi, A.H., Whitworth, T., Nowlin, W.D., 1995. On the meridional extent and fronts of the Antarctic Circumpolar Current. Deep Sea Research Part I: Oceanographic Research Papers 42, 641–673. https://doi.org/10.1016/0967-0637(95)00021-W

Pakhomov, E.A., McQuaid, C.D., 1996. Distribution of surface zooplankton and seabirds across the Southern Ocean. Polar Biology 16, 271–286. https://doi.org/10.1007/s003000050054

Park, Y.-H., Fuda, J.-L., Durand, I., Naveira Garabato, A.C., 2008. Internal tides and vertical mixing over the Kerguelen Plateau. Deep Sea Research Part II: Topical Studies in Oceanography 55, 582–593. https://doi.org/10.1016/j.dsr2.2007.12.027

Parrish, C.C., 2013. Lipids in marine ecosystems. ISRN Oceanography 2013, 604045. https://doi.org/10.5402/2013/604045

Pauthenet, E., Roquet, F., Madec, G., Guinet, C., Hindell, M., McMahon, C.R., Harcourt, R., Nerini, D., 2018. Seasonal Meandering of the Polar Front Upstream of the Kerguelen Plateau. Geophysical Research Letters 45, 9774–9781. https://doi.org/10.1029/2018gl079614

Pellichero, V., Boutin, J., Claustre, H., Merlivat, L., Sallée, J.-B., Blain, S., 2020. Relaxation of Wind Stress Drives the Abrupt Onset of Biological Carbon Uptake in the Kerguelen Bloom: A Multisensor Approach. Geophysical Research Letters 47, e2019GL085992. https://doi.org/10.1029/2019gl085992

Perissinotto, R., Duncombe Rae, C.M., 1990. Occurrence of anticyclonic eddies on the Prince Edward Plateau (Southern Ocean): effects on phytoplankton biomass and production. Deep Sea Research Part A. Oceanographic Research Papers 37, 777–793. https://doi.org/10.1016/0198-0149(90)90006-H

Pollard, R., Sanders, R., Lucas, M., Statham, P., 2007. The Crozet Natural Iron Bloom and Export Experiment (CROZEX). Deep Sea Research Part II: Topical Studies in Oceanography 54, 1905–1914. https://doi.org/10.1016/j.dsr2.2007.07.023

Pond, D.W., Atkinson, A., Shreeve, R.S., Tarling, G., Ward, P., 2005. Diatom fatty acid biomarkers indicate recent growth rates in Antarctic krill. Limnology and Oceanography 50, 732–736. https://doi.org/10.4319/lo.2005.50.2.0732

Quéroué, F., Sarthou, G., Planquette, H.F., Bucciarelli, E., Chever, F., van der Merwe, P., Lannuzel, D., Townsend, A.T., Cheize, M., Blain, S., d'Ovidio, F., Bowie, A.R., 2015. High variability of dissolved iron concentrations in the vicinity of Kerguelen Island (Southern Ocean). Biogeosciences Discuss. 12, 231–270. https://doi.org/10.5194/bgd-12-231-2015

Rembauville, M., Blain, S., Armand, L., Quéguiner, B., Salter, I., 2015a. Export fluxes in a naturally iron-fertilized area of the Southern Ocean – Part 2: Importance of diatom resting spores and faecal pellets for export. Biogeosciences 12, 3171–3195. https://doi.org/10.5194/bg-12-3171-2015

Rembauville, M., Blain, S., Manno, C., Tarling, G., Thompson, A., Wolff, G., Salter, I., 2018. The role of diatom resting spores in pelagic–benthic coupling in the Southern Ocean. Biogeosciences 15, 3071–3084. https://doi.org/10.5194/bg-15-3071-2018

Rembauville, M., Salter, I., Dehairs, F., Miquel, J.-C., Blain, S., 2017. Annual particulate matter and diatom export in a high nutrient, low chlorophyll area of the Southern Ocean. Polar Biology. https://doi.org/10.1007/s00300-017-2167-3

Rembauville, M., Salter, I., Leblond, N., Gueneugues, A., Blain, S., 2015b. Export fluxes in a naturally iron-fertilized area of the Southern Ocean – Part 1: Seasonal dynamics of particulate organic carbon export from a moored sediment trap. Biogeosciences 12, 3153–3170. https://doi.org/10.5194/bg-12-3153-2015

Remize, M., Planchon, F., Loh, A.N., Le Grand, F., Bideau, A., Le Goic, N., Fleury, E., Miner, P., Corvaisier, R., Volety, A., Soudant, P., 2020. Study of Synthesis Pathways of the Essential Polyunsaturated Fatty Acid 20:5n-3 in the Diatom Chaetoceros Muelleri Using 13C-Isotope Labeling. Biomolecules 10. https://doi.org/10.3390/biom10050797

Salter, I., Kemp, A.E.S., Moore, C.M., Lampitt, R.S., Wolff, G.A., Holtvoeth, J., 2012. Diatom resting spore ecology drives enhanced carbon export from a naturally iron-fertilized bloom in

the Southern Ocean. Global Biogeochemical Cycles 26, GB1014. https://doi.org/10.1029/2010gb003977

Salter, I., Lampitt, R.S., Sanders, R., Poulton, A., Kemp, A.E.S., Boorman, B., Saw, K., Pearce, R., 2007. Estimating carbon, silica and diatom export from a naturally fertilised phytoplankton bloom in the Southern Ocean using PELAGRA: A novel drifting sediment trap. Deep Sea Research Part II: Topical Studies in Oceanography 54, 2233–2259. https://doi.org/10.1016/j.dsr2.2007.06.008

Sargent, J.R., Eilertsen, H.C., Falk-Petersen, S., Taasen, J.P., 1985. Carbon assimilation and lipid production in phytoplankton in northern Norwegian fjords. Marine Biology 85, 109–116. https://doi.org/10.1007/BF00397428

Sassenhagen, I., Irion, S., Jardillier, L., Moreira, D., Christaki, U., 2020. Protist Interactions and Community Structure During Early Autumn in the Kerguelen Region (Southern Ocean). Protist 171, 125709. https://doi.org/10.1016/j.protis.2019.125709

Schallenberg, C., Bestley, S., Klocker, A., Trull, T.W., Davies, D.M., Gault-Ringold, M., Eriksen, R., Roden, N.P., Sander, S.G., Sumner, M., Townsend, A.T., van der Merwe, P., Westwood, K., Wuttig, K., Bowie, A., 2018. Sustained Upwelling of Subsurface Iron Supplies Seasonally Persistent Phytoplankton Blooms Around the Southern Kerguelen Plateau, Southern Ocean. Journal of Geophysical Research: Oceans 123, 5986–6003. https://doi.org/10.1029/2018jc013932

Schlosser, C., Schmidt, K., Aquilina, A., Homoky, W.B., Castrillejo, M., Mills, R.A., Patey, M.D., Fielding, S., Atkinson, A., Achterberg, E.P., 2018. Mechanisms of dissolved and labile particulate iron supply to shelf waters and phytoplankton blooms off South Georgia, Southern Ocean. Biogeosciences 15, 4973–4993. https://doi.org/10.5194/bg-15-4973-2018

Seeyave, S., Lucas, M.I., Moore, C.M., Poulton, A.J., 2007. Phytoplankton productivity and community structure in the vicinity of the Crozet Plateau during austral summer 2004/2005. Deep Sea Research Part II: Topical Studies in Oceanography 54, 2020–2044. https://doi.org/10.1016/j.dsr2.2007.06.010

Sheridan, C.C., Lee, C., Wakeham, S.G., Bishop, J.K.B., 2002. Suspended particle organic composition and cycling in surface and midwaters of the equatorial Pacific Ocean. Deep Sea Research Part I: Oceanographic Research Papers 49, 1983–2008. https://doi.org/10.1016/S0967-0637(02)00118-8

Skerratt, J.H., Nichols, P.D., McMeekin, T.A., Burton, H., 1995. Seasonal and inter-annual changes in planktonic biomass and community structure in eastern Antarctica using signature lipids. Marine Chemistry 51, 93–113. https://doi.org/10.1016/0304-4203(95)00047-U

Tang, K.W., Jakobsen, H.H., Visser, A.W., 2001. Phaeocystis globosa (Prymnesiophyceae) and the planktonic food web: Feeding, growth, and trophic interactions among grazers. Limnology and Oceanography 46, 1860–1870. https://doi.org/10.4319/lo.2001.46.8.1860

Thomson, P.G., Wright, S.W., Bolch, C.J.S., Nichols, P.D., Skerratt, J.H., McMinn, A., 2004. Antarctic distribution, pigment and lipid composition and molecular identification of the brine dinoflagellate Polarella glacialis (Dinophyceae). Journal of Phycology 40, 867–873. https://doi.org/10.1111/j.1529-8817.2004.03162.x

Trull, T.W., Davies, D.M., Dehairs, F., Cavagna, A.J., Lasbleiz, M., Laurenceau-Cornec, E.C., d'Ovidio, F., Planchon, F., Leblanc, K., Quéguiner, B., Blain, S., 2015. Chemometric perspectives on plankton community responses to natural iron fertilisation over and downstream of the Kerguelen Plateau in the Southern Ocean. Biogeosciences 12, 1029–1056. https://doi.org/10.5194/bg-12-1029-2015

Vaezi, R., Napier, J.A., Sayanova, O., 2013. Identification and functional characterization of genes encoding omega-3 polyunsaturated fatty acid biosynthetic activities from unicellular microalgae. Marine drugs 11, 5116–5129.

van der Merwe, P., Bowie, A.R., Quéroué, F., Armand, L., Blain, S., Chever, F., Davies, D., Dehairs, F., Planchon, F., Sarthou, G., Townsend, A.T., Trull, T.W., 2015. Sourcing the iron in the naturally fertilised bloom around the Kerguelen Plateau: particulate trace metal dynamics. Biogeosciences 12, 739–755. https://doi.org/10.5194/bg-12-739-2015

Venables, H., Moore, C.M., 2010. Phytoplankton and light limitation in the Southern Ocean: Learning from high-nutrient, high-chlorophyll areas. Journal of Geophysical Research: Oceans 115. https://doi.org/10.1029/2009jc005361

Virtue, P., Nichols, P.D., Nicol, S., McMinn, A., Sikes, E.L., 1993. The lipid composition of Euphausia superba Dana in relation to the nutritional value of Phaeocystis pouchetii (Hariot) Lagerheim. Antarctic Science 5, 169–177. https://doi.org/10.1017/S0954102093000239

Volkman, J.K., Barrett, S.M., Blackburn, S.I., Mansour, M.P., Sikes, E.L., Gelin, F., 1998. Microalgal biomarkers: A review of recent research developments. Organic Chemistry 29, 1163–1179. https://doi.org/10.1016/S0146-6380(98)00062-X

Wakeham, S.G., 1995. Lipid biomarkers for heterotrophic alteration of suspended particulate organic matter in oxygenated and anoxic water columns of the ocean. Deep Sea Research Part I: Oceanographic Research Papers 42, 1749–1771. https://doi.org/10.1016/0967-0637(95)00074-G

Wang, S.W., Budge, S.M., Iken, K., Gradinger, R.R., Springer, A.M., Wooller, M.J., 2015. Importance of sympagic production to Bering Sea zooplankton as revealed from fatty acid-carbon stable isotope analyses. Mar Ecol Prog Ser 518, 31–50.

Wilson, S.E., Steinberg, D.K., Chu, F.L.E., Bishop, J.K.B., 2010. Feeding ecology of mesopelagic zooplankton of the subtropical and subarctic North Pacific Ocean determined with fatty acid biomarkers. Deep Sea Research Part I: Oceanographic Research Papers 57, 1278–1294. https://doi.org/10.1016/j.dsr.2010.07.005

G. Supplementary information

Table S1. Mean fatty acid composition of phytoplankton classes reported from the meta-analysis of Jónasdóttir (2019) and Cañavate (2019) as well as the screening study of Mitani et al. (2017).

Phylum	Class	14:0	16:1n-7	18:1n-9	18:1n-7	16:2n-7	16:2n-4	16:3n-4	16:4n-1	16:4n-3	18:2n-6	18:3n-6	18:3n-3	18:4n-3	18:5n-3	20:4n-6	20:5n-3	22:6n-3
CYANOPHYTA	Cyanophyceae	2.0	9.6	6.6	4.3		1.1				**11.4**	**5.0**	**17.3**	5.1				
CHLOROPHYTA	Chlorophyceae	0.8	1.5	4.6	1.4					**14.6**	6.2	2.7	**30.8**	1.0				
	Trebouxiophyceae	1.0	3.1	4.7	1.3					0.4	**14.5**	0.6	**22.5**	1.0				
	Chlorodendrophyceae	1.0	2.0	10.7	2.8					**11.7**	6.5	0.4	**15.3**	7.0	0.9	0.6	4.8	
	Pyramimonadophyceae	1.4	2.9	1.7	3.4					**12.8**	2.6	0.6	9.1	**15.7**	**6.3**	1.9	1.1	5.1
	Prasinophycea	1.2	3.3	1.1	5.4		0.2			**15.4**	1.3	0.7	11.0	**23.7**	**7.0**		0.3	6.1
	Mamiellophyceae	**11.9**	1.4	1.4	2.3					**17.5**	1.8	0.3	9.1	**15.9**	3.2	0.7	1.2	7.0
RHODOPHYTA	Porphyridophyceae	0.8	2.2	1.1	1.9						9.4	0.6				**23.0**	**21.8**	
CRYPTOPHYTA	Cryptophyceae	6.4	2.0	3.2	3.7						4.1	0.7	**17.9**	**18.8**		1.2	9.8	5.9
HAPTOPHYTA	Coccolithophyceae	**17.6**	3.2	13.4	1.8	0.3	0.8				4.2	0.9	4.7	9.6	**5.8**	0.3	1.4	**11.6**
	Prymnesiophyceae	**18.3**	4.9	11.0	2.3	0.5	0.4				4.6	1.2	5.0	**12.0**	**7.2**	0.1	2.4	**10.7**
	Pavlovophyceae	**13.7**	**17.0**	2.1	1.4	0.3	0.7				2.2	0.9	2.1	6.2		0.9	**18.9**	8.4
DINOPHYTA	Dinophyceae	7.1	2.7	5.0	2.1					2.2	2.3	0.2	0.9	6.3	**16.1**	2.3	5.3	**17.5**
OCHROPHYTA	Eustigmatophyceae	4.2	**24.8**	5.8	0.6	0.5	0.4				3.1	0.5	0.7	0.2	0.4	3.9	23.4	
	Raphydophyceae	9.8	7.3	3.9	1.4		1.9				2.9	0.7	4.0	**12.6**	2.3	4.1	**19.0**	2.5
	Pelagophyceae	**13.7**	7.6	6.6							2.9		6.0	**13.4**	4.1		1.0	6.4
	Pinguiophycea	**22.9**	2.3	5.3	0.7						3.3	0.2	0.1	1.9	1.0	5.5	**35.8**	5.9
DIATOMA	Bacillariophyceae	9.0	**21.8**	3.0	1.2		**4.0**	**5.3**	**2.6**	1.0	2.0	0.5	1.0	0.5	0.2	3.0	**14.9**	1.0
	Cosciondiscophyceae	**14.3**	**19.5**	1.9	1.6	**2.6**	**4.1**	**9.0**	**5.5**		1.1	0.5	0.3	2.8		1.4	**18.5**	2.5
	Fragilariophyceae	**18.1**	**24.4**	2.0	1.9		**5.3**	**3.1**	**3.6**	2.4	1.5	0.0	0.9	0.5	0.1	0.3	**19.5**	1.3
	Mediophyceae	**14.6**	**15.0**	1.6		**2.0**	**4.0**	**3.3**	**9.7**		1.4		0.9	1.1		3.3	**17.1**	2.4

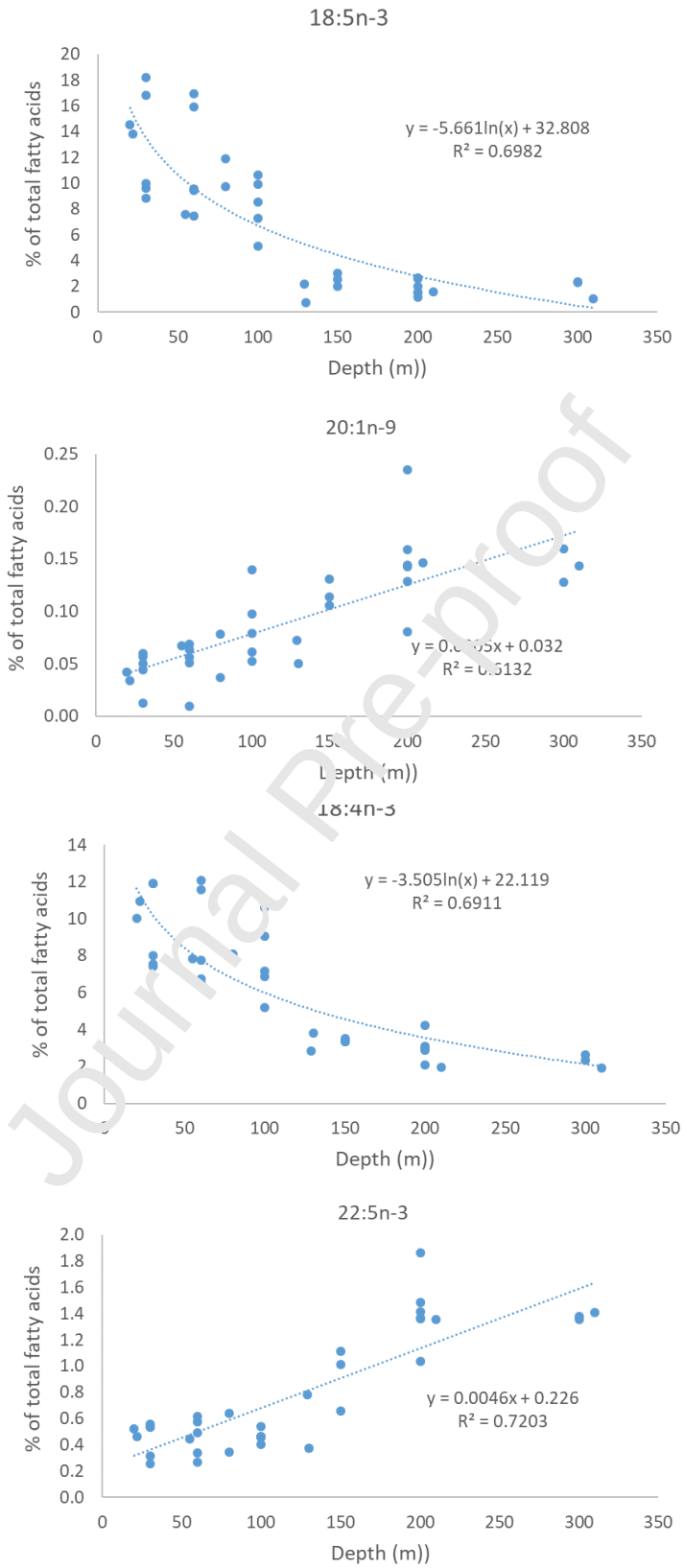

Figure S1. Most significant regressions of fatty acids variables according to depth ($p<0.0001$).

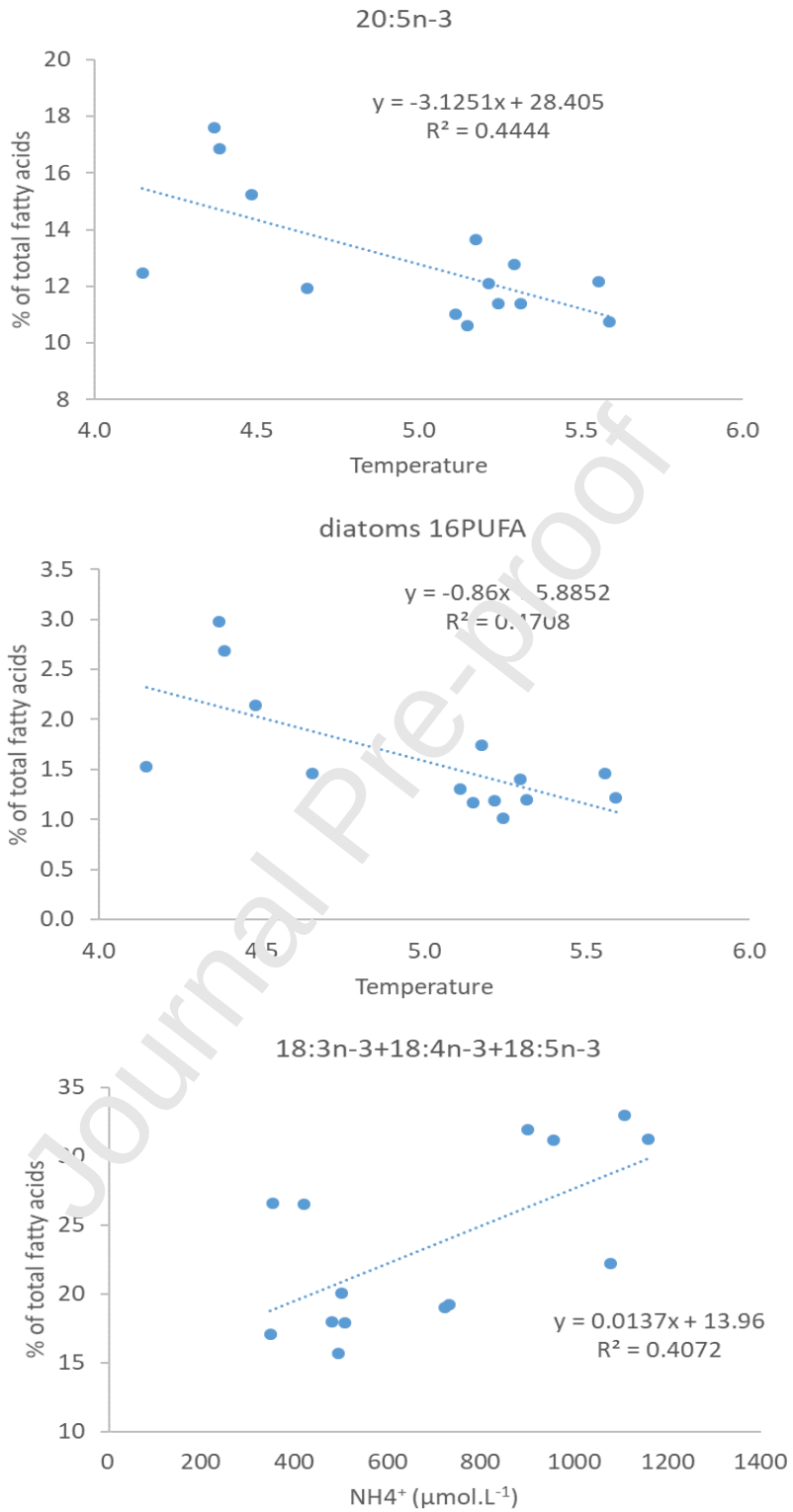

Figure S2: Most significant regressions of fatty acid variables according to physico-chemical parameters ($p<0.01$). Temperature in °C.

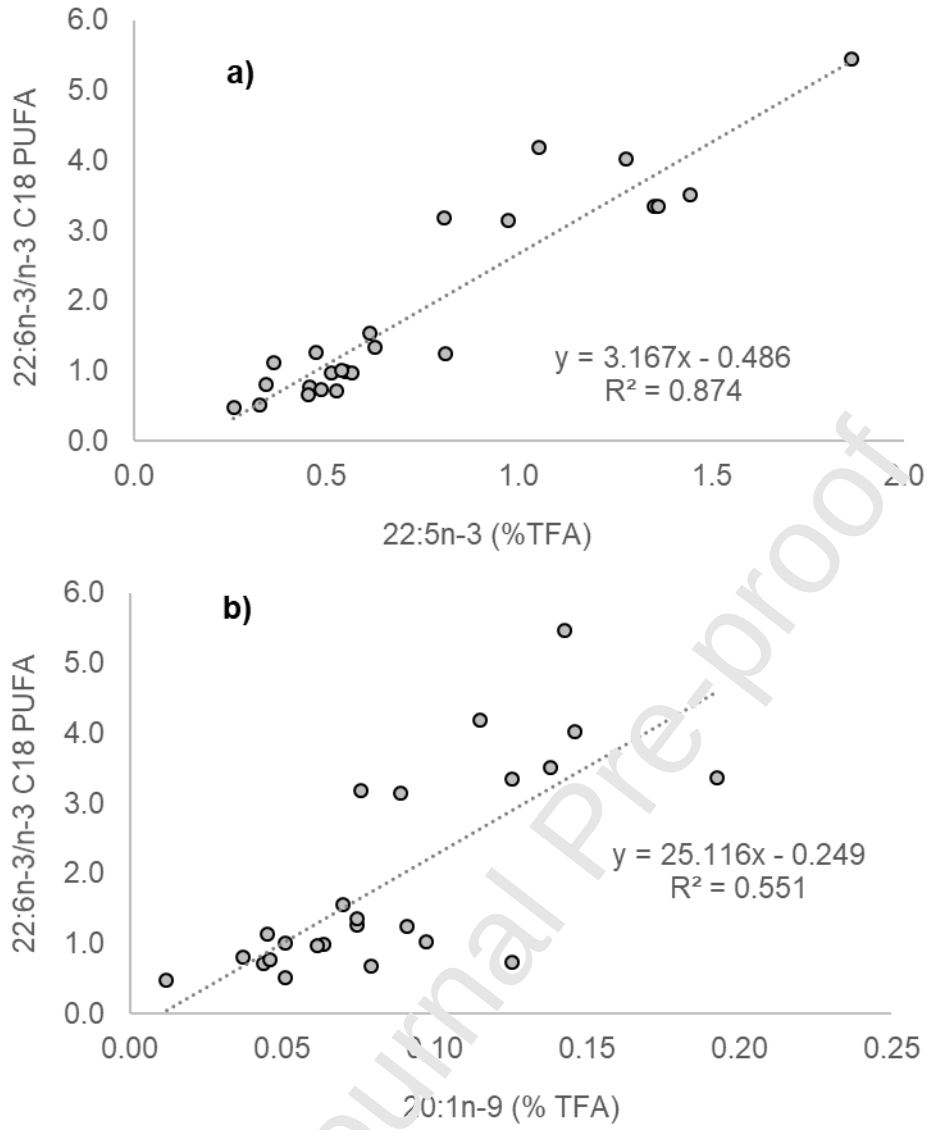

Figure S3: Relationships between 22:6n-3/n-3 C18 PUFA ratio and proportions (% TFA) of 22:5n-3 (a) and 20:1n-9 (b). Depth-weighted averaged proportions in three depth intervals (ML, MLD-150m, and 150-300m) for all stations were considered

Highlights:

- FA profiles of SPOM from the Kerguelen region during the post-bloom period was dominantly composed of PUFA with high proportions of the two LC-PUFA 20:5n-3 and 22:6n-3.
- Abundance of LC-PUFA in the mixed layer derived from the phytoplankton community composed of small species (prymnesiophytes and prasinophytes) and diatoms.
- In the upper mesopelagic, LC-PUFA are maintained at high proportions according to distinct pathways, export of diatoms for 20:5n-3 and zooplankton fecal material for 22:6n-3.
- SPOM revealed high nutritional quality in the upper water column (0-300m) both in the iron-fertilized area on the Plateau and outside in HNLC waters.